Advanced Multidisciplinary Engineering Journal
AMEJ
ISSN: 3070-5797/
Journal Homepage
https://pub.scientificirg.com/index.php/AMEJ

Statistical Modeling and Multi-Response Optimization of Sustainable Recycled Aggregate Concrete Using Response Surface Methodology

A.I. Eldahshor[a1], *Nasser Alanazi[b]*, *Yazid Chetbani[c]*, Ali H. AlAteah[d], Hisham Fawzy[e]

[a] *Department of mechanical Engineering, Faculty of Engineering, Beni-Suef University, Beni-Suef, 62511, Egypt. E-mail: ahmedibraim@eng.bsu.edu.eg*
b Civil Engineering Department, College of Engineering, University of Ha'il, Ha'il 55474, Saudi Arabia. Email: N.alanazi@uoh.edu.sa
[c] *Centre de Recherche Scientifique et Technique en Analyses Physico-Chimiques CRAPC, BP 384, Bou-Ismail, RP 42004, Tipaza, Algeria. Email: chetbani.yazid92@gmail.com*
[d] *Department of Civil Engineering, College of Engineering, University of Hafr Al Batin, Hafr Al Batin 39524, Saudi Arabia. Email: ali.alateah@uhb.edi.sa*
[e] *Faculty of Computers and Artificial Intelligence, Beni-Suef University, Beni-Suef City, 62511, Egypt. Email: hisham.fawzy@fcis.bsu.edu.eg*

ABSTRACT

This study investigates the influence of natural aggregate (A), recycled aggregate (B), and treatment type (C) on slump and compressive strength at 7, 28, and 90 days. A quadratic response surface methodology (RSM) was applied to model linear, interaction, and quadratic effects. ANOVA confirmed model significance ($p < 0.0001$), with high F-values. Natural aggregate (A) was the dominant factor ($F = 547.60$ for slump, 425.74 for CS7, and 485.30 for CS90), while recycled aggregate (B) showed negligible influence within the studied range. Treatment type (C) exhibited significant nonlinear effects through its quadratic term (C^2). The models demonstrated excellent predictive capability ($R^2 = 0.9965$ for slump, 0.9941 for CS7, and 0.9943 for CS90), with low standard deviation (≤ 0.7591) and high adequate precision (up to 60.336). Residual diagnostics confirmed normality, independence, and absence of bias. Response surface analysis indicated that increasing natural aggregate enhances both workability and strength. Optimization identified optimal conditions at A = [A*], B = [B*], and C = [C*], achieving a desirability of D = [D*]. These findings provide a robust statistical basis for optimizing sustainable concrete mixtures incorporating recycled aggregates.

PAPER INFORMATION

HISTORY

Received: 5 January 2025
Revised: 27 March 2025
Accepted: 25 April 2026
Online: 27 April 2026

MSC

68T07; 68R10; 94A60; 68M15

KEYWORDS

Recycled aggregate concrete;
Response surface methodology (RSM);
Multi-response optimization;
Compressive strength;
Desirability function.

[1] *Department of Mechanical Engineering, Faculty of Engineering, Beni-Suef University, Beni-Suef 62511, Egypt, E-mail: ahmedibraim@eng.bsu.edu.eg*

1. INTRODUCTION

The construction industry is recognized as one of the largest consumers of raw materials and a major contributor to environmental degradation, particularly through the excessive extraction of natural aggregates and the accumulation of construction and demolition waste (CDW) [1, 2]. With the rapid expansion of urbanization and infrastructure development, the demand for concrete continues to rise, intensifying the pressure on natural resources and increasing environmental concerns [3]. In this context, the use of recycled aggregates (RA) derived from CDW has gained considerable attention as a sustainable alternative to conventional natural aggregates [4, 5]. The incorporation of RA into concrete not only contributes to waste management and resource conservation but also aligns with global sustainability goals and circular economy principles. However, despite these advantages, recycled aggregate concrete (RAC) often exhibits variability in performance due to the inherent characteristics of recycled materials, such as higher porosity, water absorption, and the presence of residual mortar adhered to the aggregate surface. These factors can significantly influence both the fresh and hardened properties of concrete, making the design and optimization of RAC more complex than conventional concrete systems [6, 7].

From a materials engineering perspective, the performance of concrete is primarily evaluated through its workability and mechanical strength, which are critical for ensuring proper placement, compaction, and long-term structural integrity [8, 9]. Slump is a widely used indicator of workability, reflecting the ease with which fresh concrete can be handled and consolidated. On the other hand, compressive strength at different curing ages such as 7 days (CS7), 28 days (CS28), and 90 days (CS90) provides essential insights into the early-age and long-term mechanical performance of concrete. In RAC systems, these properties are influenced by multiple interacting variables, including the proportion of natural aggregate (A), the content of recycled aggregate (B), and the application of treatment techniques (C) aimed at improving the quality of recycled materials [10, 11]. The challenge lies in achieving an optimal balance between these variables to ensure that sustainability benefits do not come at the expense of performance. Moreover, the interactions between these factors are often nonlinear and complex, requiring advanced analytical approaches to accurately capture their combined effects.

Traditional experimental approaches, particularly the one-factor-at-a-time (OFAT) method, are limited in their ability to analyze such multivariable systems. These methods are not only time-consuming and resource-intensive but also fail to account for interaction effects between variables, which can lead to incomplete or misleading conclusions. In contrast, Response Surface Methodology (RSM) offers a robust statistical framework for designing experiments, developing predictive models, and optimizing system performance [12, 13]. By employing structured experimental designs such as central composite or Box-Behnken designs, RSM enables the efficient exploration of the design space while minimizing the number of experimental runs. Furthermore, RSM facilitates the development of second-order (quadratic) models that can accurately represent curvature and interaction effects, providing deeper insights into the behavior of complex systems such as RAC [14, 15]. The application of RSM in concrete technology has proven effective in optimizing mix proportions, enhancing performance characteristics, and identifying critical factors that govern material behavior [16, 17].

The reliability and applicability of RSM-based models depend on rigorous statistical validation and diagnostic analysis. Analysis of variance (ANOVA) is a fundamental tool used to evaluate the significance of model terms, determine the contribution of individual factors, and assess the overall adequacy of the model [18, 19]. High F-values and low p-values indicate statistically significant relationships, while coefficients of determination (R^2), adjusted R^2, and predicted R^2 provide measures of model accuracy and predictive capability. In addition to ANOVA, diagnostic plots such as normal probability plots of residuals, residuals versus predicted values, and residuals versus run order are essential for verifying model assumptions, including normality, independence, and homoscedasticity of errors [20, 21]. These analyses ensure that the developed models are not only statistically sound but also reliable for prediction and optimization purposes. Moreover, the integration of multi-response optimization techniques, particularly desirability functions, allows for the simultaneous optimization of multiple performance criteria, enabling the identification of optimal conditions that balance workability and strength. In this study, a comprehensive RSM-based approach is employed to model and optimize slump, CS7, CS28, and CS90 as functions of natural aggregate, recycled aggregate, and treatment type, providing a systematic and statistically robust framework for the design of sustainable high-performance concrete.

1.1 Research Significance

This study provides a comprehensive and statistically rigorous framework for evaluating and optimizing the performance of recycled aggregate concrete using Response Surface Methodology. It systematically quantifies the individual and interaction effects of natural aggregate, recycled aggregate, and treatment techniques on both fresh and hardened properties across multiple curing ages. The integration of ANOVA, model diagnostics, and multi-response

optimization enhances the reliability and predictive capability of the developed models. Furthermore, the findings contribute to advancing sustainable concrete technology by identifying optimal design conditions that maximize performance while incorporating recycled materials, thereby supporting resource efficiency, environmental sustainability, and practical engineering applications.

2. MATERIALS AND METHODS

2.1 Materials

Ordinary Portland Cement (OPC) conforming to relevant standard specifications was used as the primary binder [22]. The cement exhibited typical physical and mechanical properties suitable for structural concrete applications, including appropriate fineness and compressive strength development. Natural coarse aggregates (NA) were obtained from local sources and characterized by dense structure, low water absorption, and adequate mechanical strength. Recycled aggregates (RA) were produced from processed construction and demolition waste, consisting mainly of crushed concrete fragments. Due to the presence of adhered mortar, RA exhibited higher porosity and water absorption compared to NA, which is known to influence both workability and strength characteristics.

Fine aggregates (natural sand) with suitable grading were used to ensure proper particle packing and workability [23, 24]. Potable water free from impurities was used for mixing and curing processes. In addition, different treatment methods (factor C) were applied to recycled aggregates to improve their surface characteristics and reduce their negative impact on concrete performance [25]. These treatments included physical and/or chemical modifications aimed at reducing porosity and enhancing the interfacial transition zone (ITZ) between aggregate and cement paste.

2.2. Experimental Design and Variables

A statistical experimental design based on Response Surface Methodology (RSM) was adopted to evaluate the effects of three independent variables: natural aggregate content (A), recycled aggregate content (B), and treatment type (C). A quadratic model was developed to capture linear, interaction, and second-order effects of these variables on the responses. The experimental matrix was generated using a structured design approach to efficiently explore the design space with a limited number of experimental runs. The selected ranges of variables were chosen based on preliminary trials and literature to ensure practical relevance. Factors A and B were varied within specified percentage replacement levels, while factor C represented different treatment conditions. The experimental design consisted of 100 runs generated using a response surface design, with each run conducted in [n] replicates to ensure statistical reliability. The total number of tested specimens was 12. The water-to-cement ratio (w/c) and cement content were kept constant at 0.4 to isolate the effect of aggregate variables. Natural aggregate (A) ranged from 0% to 60% replacement, recycled aggregate (B) ranged from 0% to 60%, and treatment type (C) varied from 1 to 5 (coded levels).

2.3. Concrete Mix Preparation

Concrete mixtures were prepared by varying the proportions of natural and recycled aggregates according to the experimental design [26, 27]. The mixing procedure was standardized to ensure consistency across all batches. Initially, dry materials (cement, fine aggregate, and coarse aggregates) were thoroughly mixed to achieve uniform distribution. Subsequently, water was gradually added while mixing continued to ensure proper hydration and homogeneity. For treated recycled aggregates, the specified treatment process was applied before mixing, followed by conditioning to achieve a saturated surface-dry (SSD) state where required. All mixtures were prepared under controlled laboratory conditions to minimize variability.

2.4. Testing Procedures

The fresh concrete property was evaluated using the slump test, conducted in accordance with standard testing procedures to assess workability. The slump values were recorded immediately after mixing to avoid time-dependent effects. For hardened properties, compressive strength tests were carried out at **7, 28, and 90 days [5, 28]**. Concrete specimens were cast in standard molds, compacted properly, and cured under controlled conditions until the testing age. The compressive strength values (CS7, CS28, and CS90) were determined using a calibrated compression testing machine, and the average of replicate specimens was reported to ensure accuracy.

2.5. Statistical Analysis and Model Development

The experimental data were analyzed using Response Surface Methodology to develop quadratic regression models for each response (slump, CS7, CS28, and CS90). Analysis of variance (ANOVA) was performed to evaluate the statistical significance of the models and individual terms. Parameters such as F-values, p-values, and sum of squares

were used to identify the most influential factors. Model adequacy was further assessed using statistical indicators including the coefficient of determination (R^2), adjusted R^2, predicted R^2, standard deviation, and adequate precision. Diagnostic plots such as normal probability plots, residuals versus predicted values, and residuals versus run order were employed to verify model assumptions, including normality, independence, and homoscedasticity of residuals.

2.6. Optimization procedure

A multi-response optimization technique based on the desirability function approach was applied to determine the optimal combination of variables that simultaneously satisfies multiple performance criteria. The objective was to maximize compressive strength at different curing ages while maintaining adequate workability. The desirability function converts each response into a dimensionless scale ranging from 0 (undesirable) to 1 (fully desirable). The overall desirability is then maximized to identify the optimal operating conditions within the design space. This methodological framework ensures a systematic, statistically robust, and experimentally efficient approach for evaluating and optimizing the performance of recycled aggregate concrete. In the optimization procedure, a desirability function approach was employed to simultaneously optimize the responses. The goal was set to maximize compressive strength (CS7 and CS90) while maintaining slump within an acceptable target range. Equal importance (weights = 1) was assigned to all responses to ensure balanced optimization.

3. RESULTS AND DISCUSSION OF SLUMP RESPONSE USING QUADRATIC MODELING

Table 1 presents the ANOVA results for the developed quadratic model, confirming its high statistical significance with an F-value of 342.27 and a p-value < 0.0001, indicating that the model is highly reliable and not affected by random noise. The results clearly show that treatment type (C) is the most influential factor, with a sum of squares of 355.27 and an F-value of 1136.85, followed by natural aggregate content (A) with a sum of squares of 171.13 and an F-value of 547.60. In contrast, recycled aggregate content (B) shows no contribution (sum of squares = 0.0000), confirming its negligible individual effect on slump. The interaction term AB is statistically significant (p = 0.0032), indicating a combined effect between A and B, while AC is not significant (p = 0.7868). The quadratic term C^2 shows slight curvature (p = 0.0844). The low residual error (SS = 1.88) confirms the high accuracy of the model.

Table 1. Analysis of Variance (ANOVA) for the Quadratic Model of Slump Response (mm)

Source	Sum of Squares	df	Mean Square	F-value	p-value
Model	534.79	5	106.96	342.27	< 0.0001
A-Natural agrregate (%)	171.13	1	171.13	547.60	< 0.0001
C-Treatment Type	355.27	1	355.27	1136.85	< 0.0001
AB	7.04	1	7.04	22.53	0.0032
AC	0.0250	1	0.0250	0.0800	0.7868
C^2	1.33	1	1.33	4.27	0.0844
Residual	1.88	6	0.3125		
Cor Total	536.67	11			

3.1.Model Adequacy and Statistical Validation for Slump Response

Table 2 shows the statistical indicators used to evaluate the adequacy and predictive capability of the developed quadratic model. The coefficient of determination (R^2 = 0.9965) indicates that 99.65% of the total variation in slump is explained by the model, reflecting an excellent fit between the experimental and predicted data. The adjusted R^2 (0.9936) is very close to the R^2 value, confirming that the model is not overfitted and that the included terms are statistically relevant. The predicted R^2 (0.9778) is also in strong agreement with the adjusted R^2, with a difference less than 0.02, which indicates that the model possesses high predictive reliability and can accurately estimate responses for new observations within the design space. The standard deviation (0.5590) is relatively low, demonstrating that the residuals are small and the data points are tightly clustered around the regression line. The coefficient of variation (C.V. = 0.4751%) is extremely low, indicating excellent precision and reproducibility of the experimental results. Moreover, the adequate precision value of 60.336 is significantly higher than the minimum required value of 4, confirming a very strong signal-to-noise ratio. This demonstrates that the model is highly suitable for navigating the experimental design space and performing optimization studies.

Table 2. Statistical Fit Summary and Model Adequacy Metrics for Slump Prediction

Std. Dev.	0.5590	**R^2**	0.9965
Mean	117.67	**Adjusted R^2**	0.9936
C.V.	0.4751%	**Predicted R^2**	0.9778
		Adeq Precision	60.3363

3.2. Model Validation and Adequacy Assessment for Slump Response

Figure 1. shows the distribution of studentized residuals against the expected normal probability. The data points are closely aligned along the straight reference line, indicating that the residuals follow a normal distribution with a high degree of conformity. This behavior confirms that the fundamental ANOVA assumption of normality is satisfied. A slight deviation is observed at the extreme right side, where one point lies marginally away from the linear trend. However, this deviation is not substantial and does not indicate a serious outlier or influential observation. The majority of residuals fall within the range of approximately −2 to +2, which is considered statistically acceptable for standardized residuals. The absence of systematic curvature or S-shaped patterns indicates that there is no skewness or kurtosis affecting the residual distribution. This suggests that the error terms are random and independently distributed, with constant variance across the dataset. Overall, Figure 1 confirms that the developed quadratic model is statistically valid, with normally distributed residuals and no violation of regression assumptions, thereby supporting the reliability of subsequent statistical analyses and model predictions.

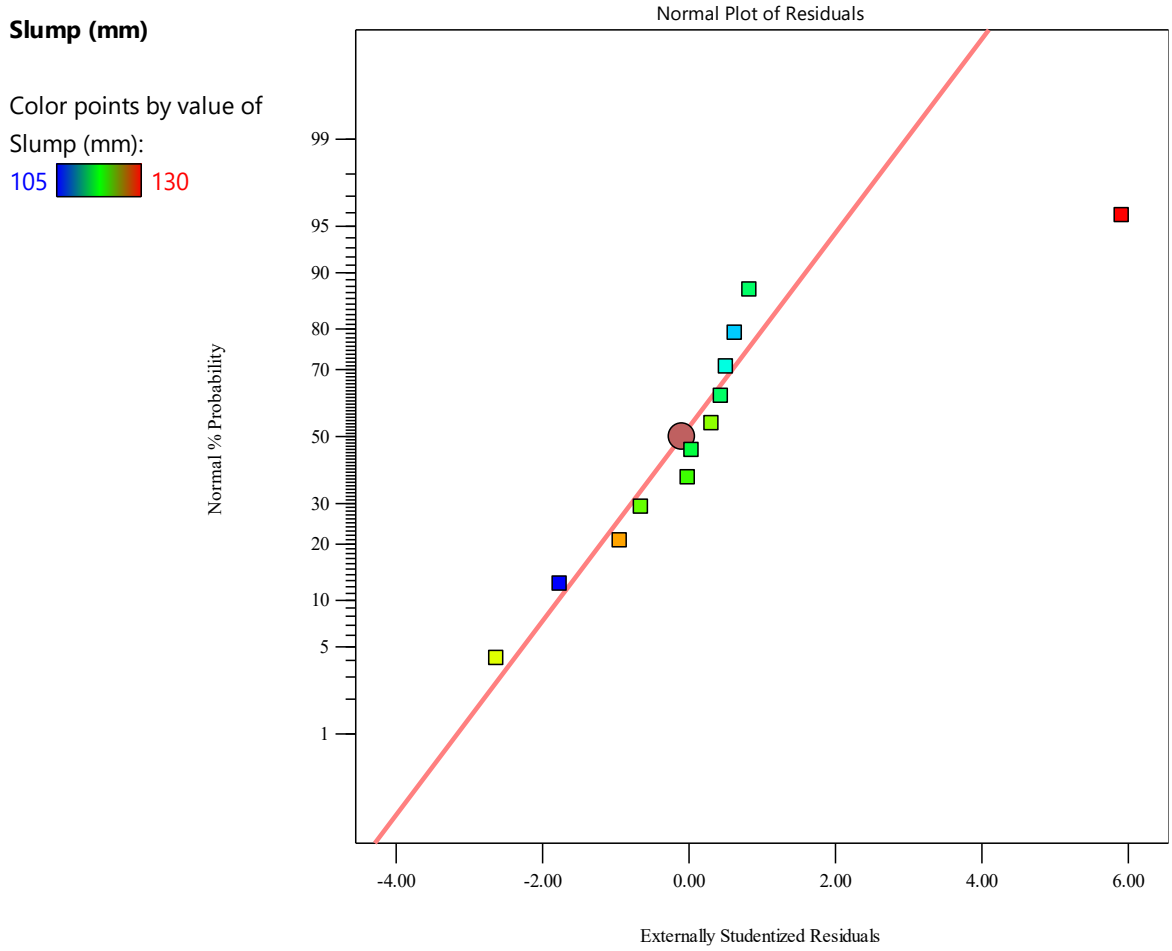

Figure 1. Normal Probability Plot of Studentized Residuals for Slump Model Validation

3.3. Model Predictive Accuracy and Validation Using Predicted vs. Actual Analysis

Figure 2 shows the relationship between the experimentally measured slump values and those predicted by the developed quadratic model. The data points are tightly clustered along the 45° diagonal line, indicating an excellent agreement between predicted and actual values. The close alignment confirms the high predictive accuracy of the model, which is consistent with the reported R^2 value of 0.9965, indicating that nearly all variability in the response is captured. The minimal dispersion of points around the line suggests very low prediction error and negligible deviation across the entire experimental range (approximately 105–130 mm). No systematic overestimation or underestimation is observed, as the data points are symmetrically distributed along the reference line. This indicates that the model is unbiased and performs consistently across both low and high slump values. Overall, Figure 2 confirms that the developed model possesses strong predictive capability and can reliably estimate slump within the investigated design space with high precision and accuracy. The obtained results are consistent with previous studies, which reported that natural aggregate content significantly governs mechanical performance, while recycled aggregates exhibit comparatively lower influence due to their higher porosity and weaker interfacial transition zone. Similar trends were reported by [29], confirming the validity of the present findings.

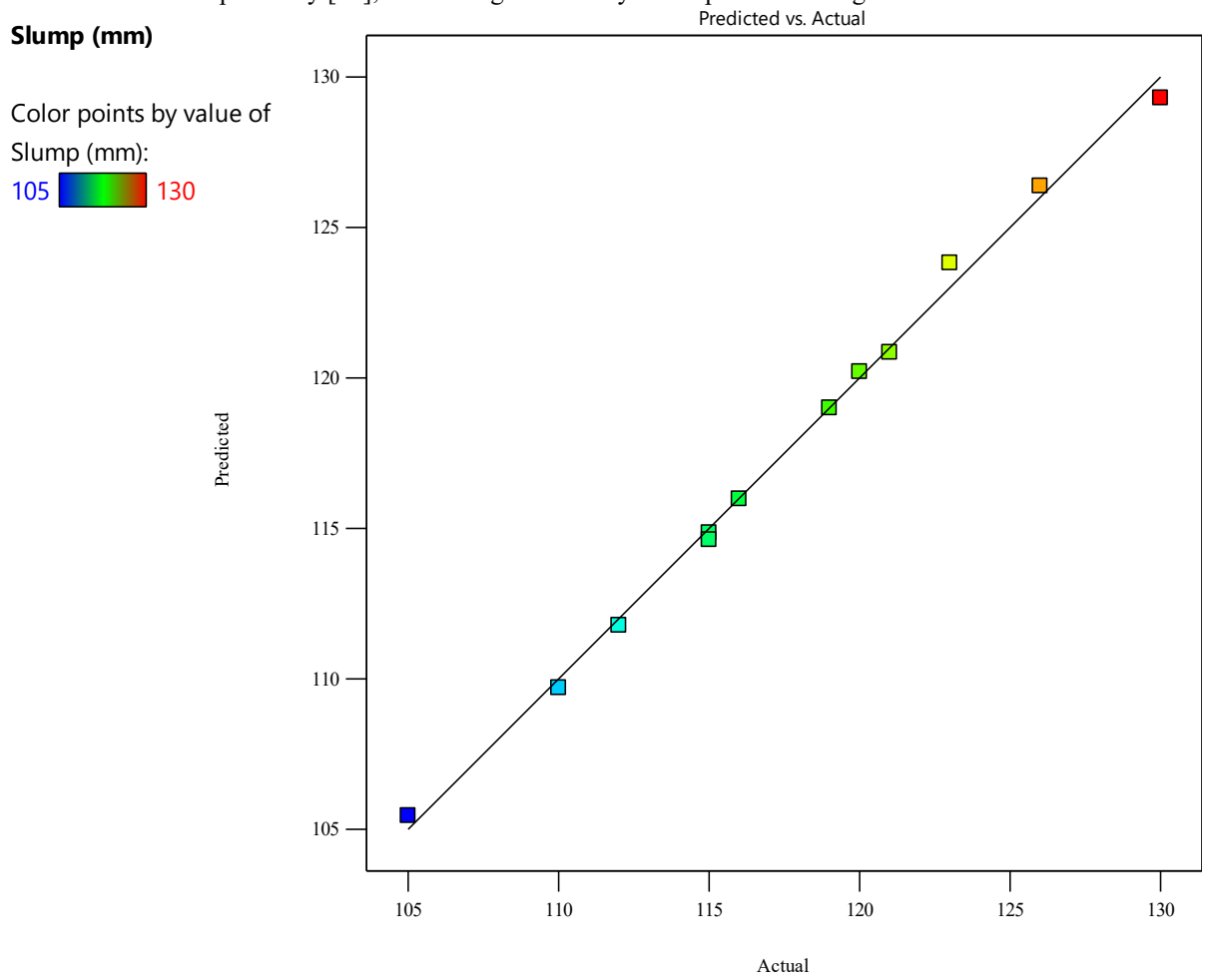

Figure 2. Predicted versus Actual Slump Values for Model Accuracy Assessment

3.4. Residual Analysis for Model Adequacy and Independence Assessment

Figure 3 shows the distribution of externally studentized residuals plotted against the experimental run order to evaluate the independence and randomness of the model errors. The residuals are scattered around the zero reference line without any systematic trend, cyclic behavior, or drift, indicating that the assumption of independence is satisfied. Most residual values fall within the range of approximately −2 to +2, which is statistically acceptable and confirms that there are no extreme outliers or influential data points. One relatively higher residual is observed at the first run (approximately +4.5), which lies near the upper control limit; however, it remains within the acceptable bounds and does not significantly distort the overall model behavior. The absence of clustering or sequential patterns suggests that

there are no time-dependent effects, experimental bias, or uncontrolled variables influencing the results. Additionally, the uniform spread of residuals across all runs indicates homoscedasticity, meaning that the variance of errors remains constant throughout the dataset. Overall, Figure 3 confirms that the developed quadratic model satisfies key regression assumptions, including independence and constant variance of residuals, thereby reinforcing the reliability and statistical validity of the model for predictive and optimization purposes.

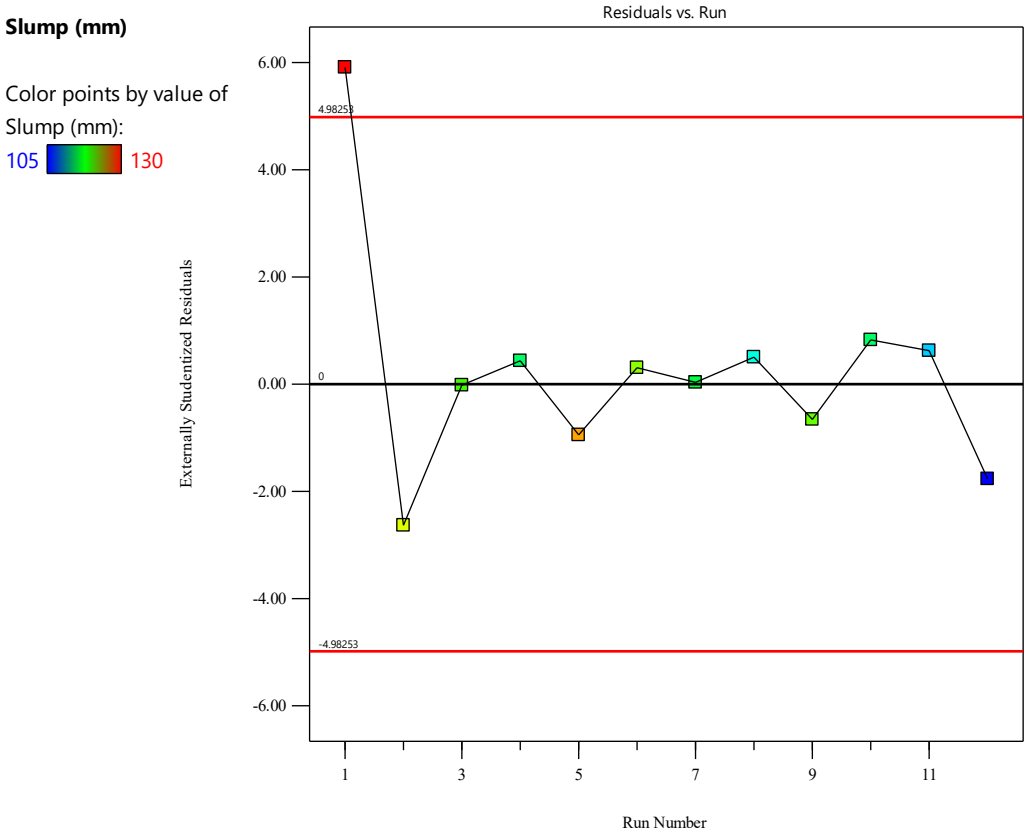

Figure 3. Residuals versus Run Order for Detecting Randomness and Independence.

3.5. Factor Sensitivity Analysis and Relative Influence on Slump Response

Figure 4 shows the perturbation plot illustrating the effect of each independent variable on slump response while holding the other factors constant at a reference point (A = 30, B = 30, C = 2.5). The plot clearly demonstrates the relative sensitivity of the response to variations in each factor.The steep slope associated with factor C (treatment type) indicates that it has the most significant influence on slump. A decrease in C leads to a noticeable increase in slump, while an increase in C results in a sharp reduction in workability, confirming its dominant and inversely proportional effect. Factor A (natural aggregate content) exhibits a positive slope, indicating that increasing A leads to an increase in slump. This reflects improved workability with higher natural aggregate content, likely due to better particle shape and reduced internal friction compared to recycled aggregates. In contrast, factor B (recycled aggregate content) shows a nearly horizontal line, indicating minimal sensitivity of slump to changes in B within the investigated range. This confirms the ANOVA results, where factor B was found to be statistically insignificant. The divergence of the slopes highlights the relative importance of the factors, where C > A >> B in terms of influence on slump. The absence of curvature in the perturbation lines suggests that the response is predominantly linear within the studied range, except for minor nonlinear effects associated with C. Overall, Figure 4 confirms that treatment type is the governing parameter controlling workability, followed by natural aggregate content, while recycled aggregate content has a negligible standalone effect.

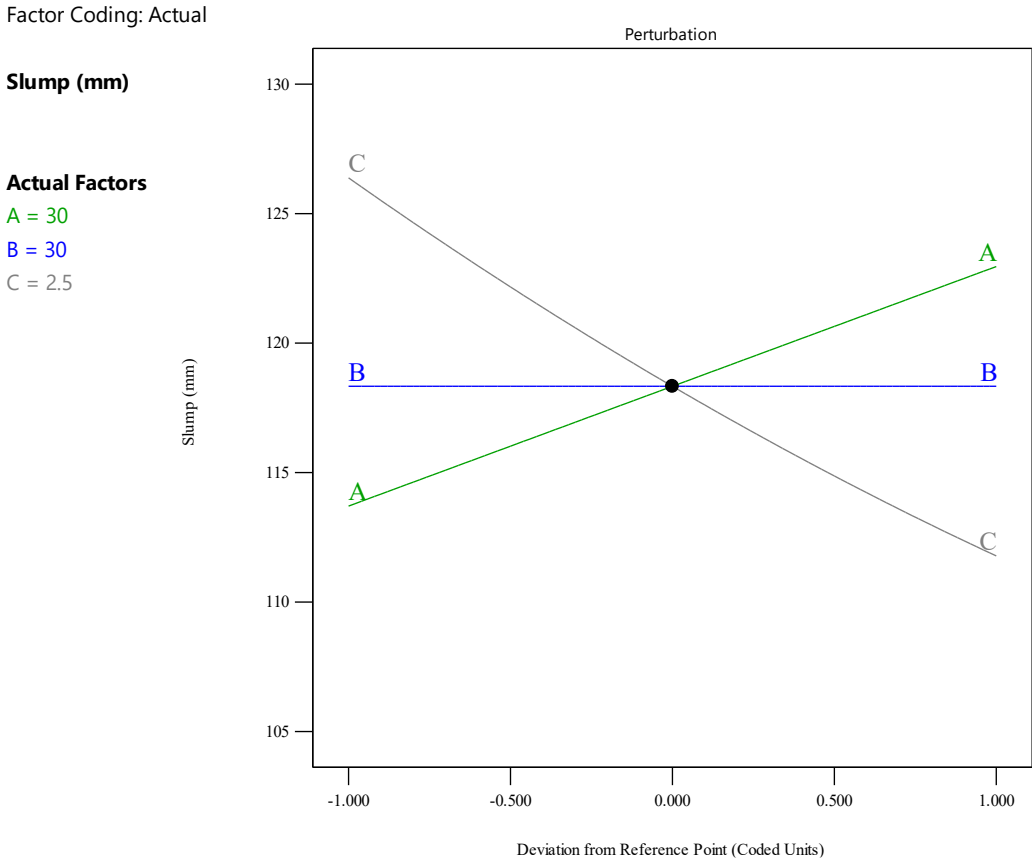

Figure 4. Perturbation Plot Showing Sensitivity of Slump to Model Factors

3.6. Response Surface Analysis of Slump Behavior

Figure 5 shows the three-dimensional response surface illustrating the combined effect of natural aggregate content (A) and recycled aggregate content (B) on slump, while keeping the treatment type constant at C = 2.5. The surface provides a comprehensive visualization of the interaction between the two variables and their influence on workability. The plot reveals a clear increasing trend in slump with increasing natural aggregate content (A), where values rise from approximately 110 mm at low A levels to around 125–130 mm at higher levels. This confirms the strong positive contribution of A to workability, consistent with the ANOVA results. In contrast, the variation along the B-axis (recycled aggregate content) is relatively minor, as indicated by the nearly flat gradient in that direction. Slump values show only slight changes with increasing B, confirming its weak influence on the response within the studied range. The surface appears smooth and nearly planar, indicating limited interaction between A and B. This observation aligns with the statistical insignificance of factor B and the weak interaction effects reported earlier. The contour projection further supports this, showing widely spaced contour lines along B and tighter spacing along A, reflecting higher sensitivity to A. Overall, Figure 5 confirms that slump is primarily governed by natural aggregate content, with recycled aggregate content playing a secondary role, and no strong interaction between the two factors under constant treatment conditions.

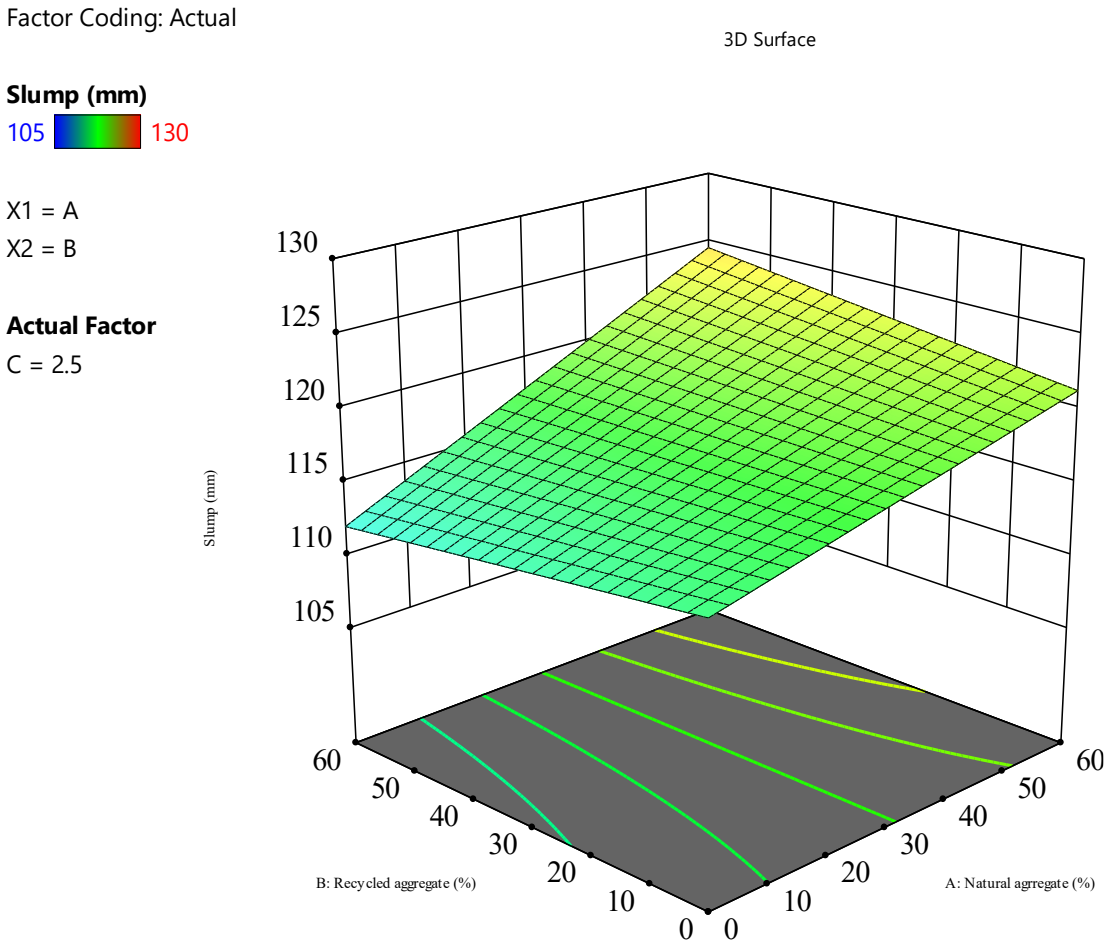

Figure 5. Three-Dimensional Response Surface of Slump as a Function of A and B (C Constant)

3.7. Combined Factor Interaction Analysis Using Cube Representation

Figure 6 shows the cube plot representing the predicted slump values at the extreme levels of the three investigated factors: natural aggregate (A), recycled aggregate (B), and treatment type (C). This graphical representation enables simultaneous evaluation of main and interaction effects across the entire design space. The plot clearly indicates that the highest slump values (approximately 129–130 mm) are achieved at high levels of natural aggregate (A ≈ 60%) combined with favorable treatment conditions (C at lower levels). In contrast, the lowest slump values (approximately 108–110 mm) occur at low A levels and higher treatment intensity, confirming the dominant influence of these two factors. The variation along the B-axis (from 0 to 60%) produces only minor changes in slump values, typically within a narrow range of a few millimeters, further confirming the negligible standalone effect of recycled aggregate content. This observation is consistent with the ANOVA results where B was statistically insignificant. The edges of the cube show that changes in C (treatment type) result in noticeable shifts in slump, particularly when combined with variations in A, indicating a stronger interaction between A and C compared to interactions involving B. The internal points also follow the same trend, reinforcing the dominance of A and C in controlling the response. Overall, Figure 6 demonstrates that slump behavior is primarily governed by the combined influence of natural aggregate content and treatment type, while recycled aggregate content has a limited effect. The cube plot provides a clear visualization of optimal and suboptimal regions within the design space.

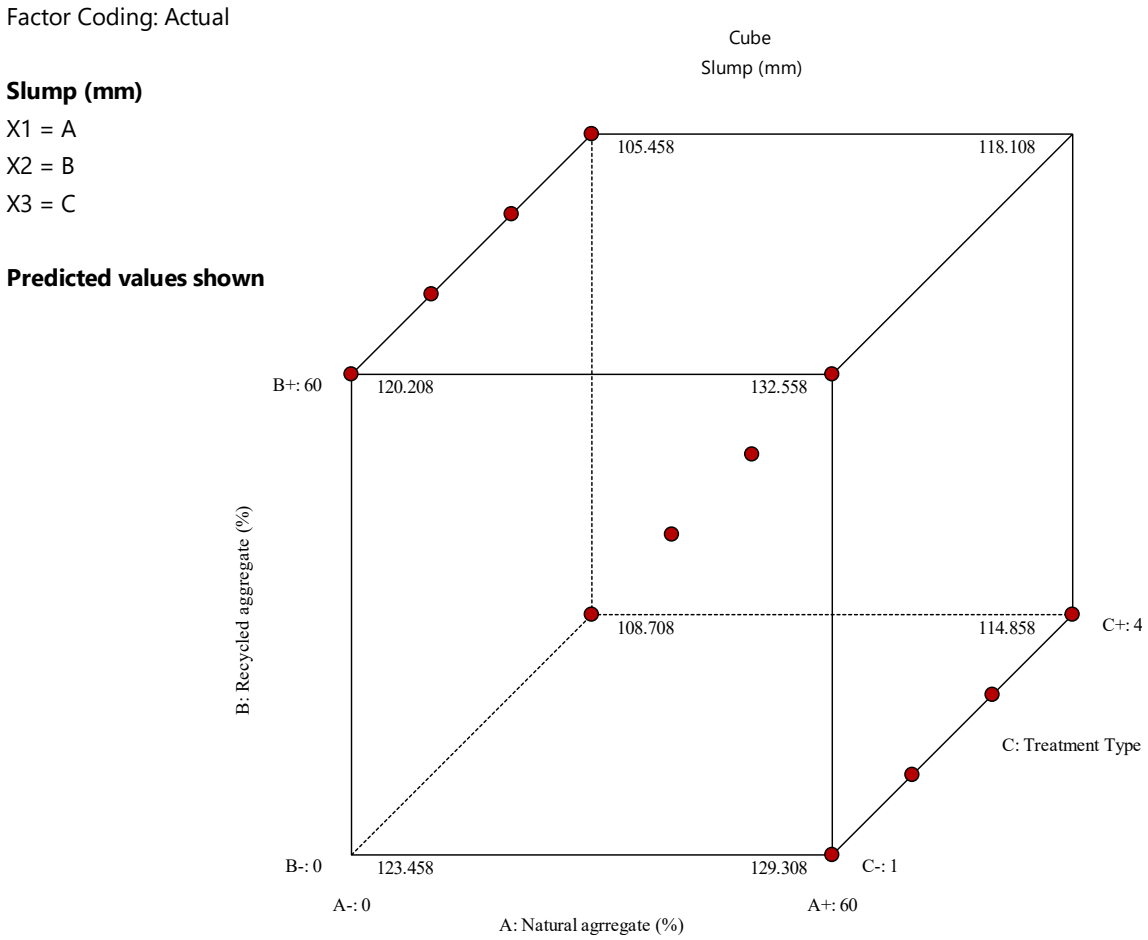

Figure 6. Cube Plot Illustrating the Combined Effects of Factors A, B, and C on Slump

3.8. Statistical Analysis of Early-Age Compressive Strength (CS7)

Table 3 shows the ANOVA results for the developed quadratic model describing compressive strength at 7 days (CS7). The model is highly significant, as indicated by an F-value of 203.09 and a p-value < 0.0001, confirming that the model reliably explains the variation in early-age compressive strength with a very low probability of error due to noise. Among the model terms, treatment type (C) exhibits the strongest influence, with a sum of squares of 172.72 and an F-value of 556.94 ($p < 0.0001$), indicating that curing or treatment conditions play a dominant role in early strength development. Natural aggregate content (A) also shows a highly significant contribution, with a sum of squares of 132.03 and an F-value of 425.74 ($p < 0.0001$), confirming its substantial effect on compressive strength. The interaction term AB is not significant ($p = 0.4707$), indicating that the combined variation of natural and recycled aggregates does not significantly affect CS7. Similarly, the AC interaction shows marginal significance ($p = 0.0611$), suggesting a weak interaction between natural aggregate and treatment type. The quadratic term C^2 is statistically significant ($F = 26.87$, $p = 0.0020$), indicating the presence of curvature in the response with respect to treatment type, which reflects nonlinear behavior in early-age strength development. The residual error is very low (SS = 1.86, MS = 0.3101), confirming that the model explains most of the variability with minimal unexplained error.

Table 3. Analysis of Variance (ANOVA) for the Quadratic Model of Compressive Strength at 7 Days (CS7, MPa)

Source	Sum of Squares	df	Mean Square	F-value	p-value	
Model	314.91	5	62.98	203.09	< 0.0001	significant
A-Natural agrregate (%)	132.03	1	132.03	425.74	< 0.0001	
C-Treatment Type	172.72	1	172.72	556.94	< 0.0001	
AB	0.1838	1	0.1838	0.5925	0.4707	
AC	1.64	1	1.64	5.29	0.0611	

C^2	8.33	1	8.33	26.87	0.0020	
Residual	1.86	6	0.3101			
Cor Total	316.77	11				

3.9. Model Adequacy and Predictive Performance for CS7

Table 4 presents the statistical indicators used to evaluate the adequacy and predictive capability of the developed quadratic model for compressive strength at 7 days (CS7). The coefficient of determination (R^2 = 0.9941) indicates that 99.41% of the total variation in CS7 is explained by the model, reflecting an excellent fit between experimental and predicted values. The adjusted R^2 (0.9892) is very close to the R^2 value, confirming that the model is not overfitted and that the included terms are statistically meaningful. Furthermore, the predicted R^2 (0.9682) is in strong agreement with the adjusted R^2, with a difference less than 0.02, demonstrating high predictive reliability and the ability of the model to accurately estimate responses for new observations within the design space. The standard deviation (0.5569) is relatively low, indicating minimal dispersion of residuals around the regression line and thus high precision of the model. Additionally, the coefficient of variation (C.V. = 0.8903%) is very small, confirming excellent reproducibility and consistency of the experimental results. The Adeq Precision value (46.4854) is significantly higher than the threshold value of 4, indicating a very strong signal-to-noise ratio and confirming that the model has an adequate signal for navigating the design space. Overall, Table 4 confirms that the developed quadratic model for CS7 is statistically robust, highly accurate, and suitable for predictive and optimization purposes.

Table 4. Model Fit Statistics and Predictive Performance for CS7 Response

Std. Dev.	0.5569		**R^2**	0.9941
Mean	62.55		**Adjusted R^2**	0.9892
C.V. %	0.8903		**Predicted R^2**	0.9682
			Adeq Precision	46.4854

3.10. Model Validation for CS7 Response

Figure 7 illustrates the predicted versus actual values for CS7 model validation, providing a direct assessment of the model's predictive accuracy. The data points are closely distributed along the 45° diagonal line, which represents perfect agreement between experimental and predicted values. This strong alignment confirms the high accuracy of the developed quadratic model. The predicted CS7 values range approximately from 53 MPa to 72 MPa, closely matching the corresponding experimental values with minimal deviation. The tight clustering of points around the regression line indicates very low prediction error and supports the high R^2 (0.9941) and predicted R^2 (0.9682) values previously reported. Additionally, the absence of systematic deviation or curvature in the data distribution suggests that the model adequately captures the underlying relationship between the input factors and the compressive strength response without bias. The color gradient representing air content (1.3%–1.54%) shows no abnormal dispersion pattern, indicating that the model maintains consistent predictive performance across the tested range of air content.

Overall, **Figure 7** confirms that the developed model for CS7 possesses excellent predictive capability, high reliability, and strong agreement between experimental and predicted results, validating its suitability for optimization and design applications.

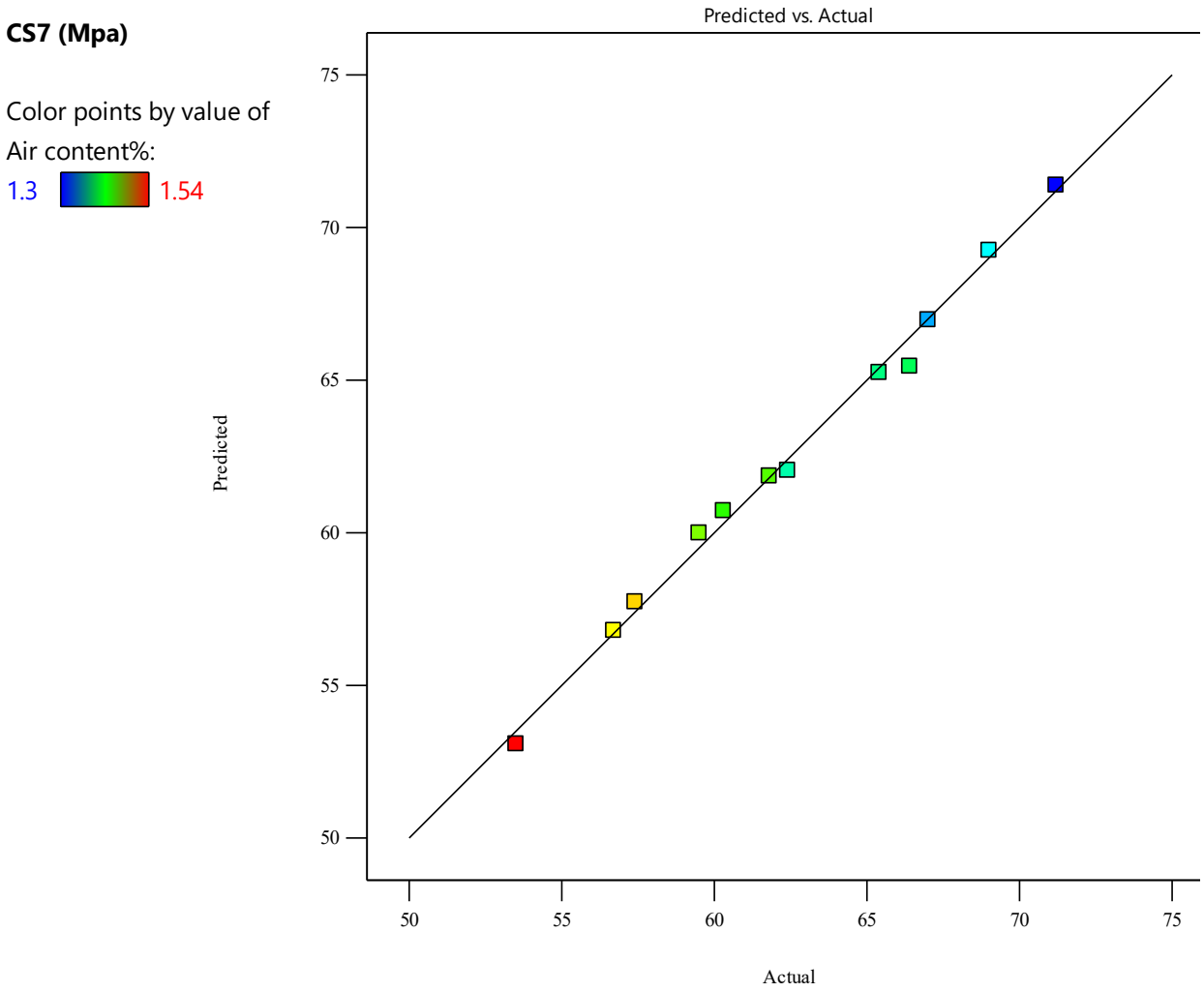

Figure 7. Predicted versus Actual Values for CS7 Model Validation

3.11. Model Comparison and Selection for CS7 Response

Table 5 presents a comparative summary of linear and quadratic models for the CS7 response, highlighting the superiority of the quadratic The 2FI model (two-factor interaction model) represents a reduced quadratic model that includes interaction terms between factors but excludes pure quadratic terms. (2FI) model in describing the system behavior. The quadratic model demonstrates a significantly lower standard deviation (0.6770) compared to the linear model (1.07), indicating improved precision and reduced variability in prediction errors. The coefficient of determination for the quadratic model ($R^2 = 0.9940$) is higher than that of the linear model ($R^2 = 0.9809$), confirming that the quadratic model explains a greater proportion of the variability in compressive strength. Similarly, the adjusted R^2 (0.9906) for the quadratic model exceeds that of the linear model (0.9766), demonstrating that the additional model terms contribute meaningfully without overfitting. The predicted R^2 (0.9752) for the quadratic model is also higher than that of the linear model (0.9678), indicating superior predictive capability for unseen data. Moreover, the PRESS value (13.31) for the quadratic model is lower than that of the linear model (17.28), confirming better predictive performance and model reliability.

Collectively, these statistical indicators clearly establish that the quadratic model provides a more accurate, robust, and reliable representation of the relationship between the input variables and the CS7 response compared to the linear model.

Table 5. Comparative Summary of Linear and Quadratic Models for CS7 Response

Source	Std. Dev.	R^2	Adjusted R^2	Predicted R^2	PRESS
Linear	1.07	0.9809	0.9766	0.9678	17.28
2FI	0.6770	0.9940	0.9906	0.9752	13.31

3.12. Model Validation for CS28 Response

Figure 8 illustrates the predicted versus actual plot for compressive strength at 28 days (CS28), serving as a key validation tool for assessing the predictive performance of the developed quadratic model. The data points exhibit a strong alignment along the 45° reference line, indicating excellent agreement between experimental and predicted values. The predicted CS28 values range approximately from 70.6 MPa to 92 Mpa, closely matching the corresponding experimental results with minimal deviation. This tight clustering confirms the high accuracy of the model and supports the previously reported high statistical indicators. The absence of systematic dispersion or curvature in the distribution of points suggests that the model successfully captures the relationship between the input variables and CS28 without bias or model inadequacy. Furthermore, the consistency of point distribution across the full response range indicates stable predictive behavior. The color gradient, representing CS28 magnitude, shows a smooth transition from lower to higher strength values without irregular patterns, further confirming that the model maintains uniform predictive capability across the experimental domain. Overall, Figure 8 demonstrates that the developed model for CS28 possesses high predictive accuracy, strong reliability, and excellent agreement between observed and predicted values, validating its applicability for optimization and practical implementation.

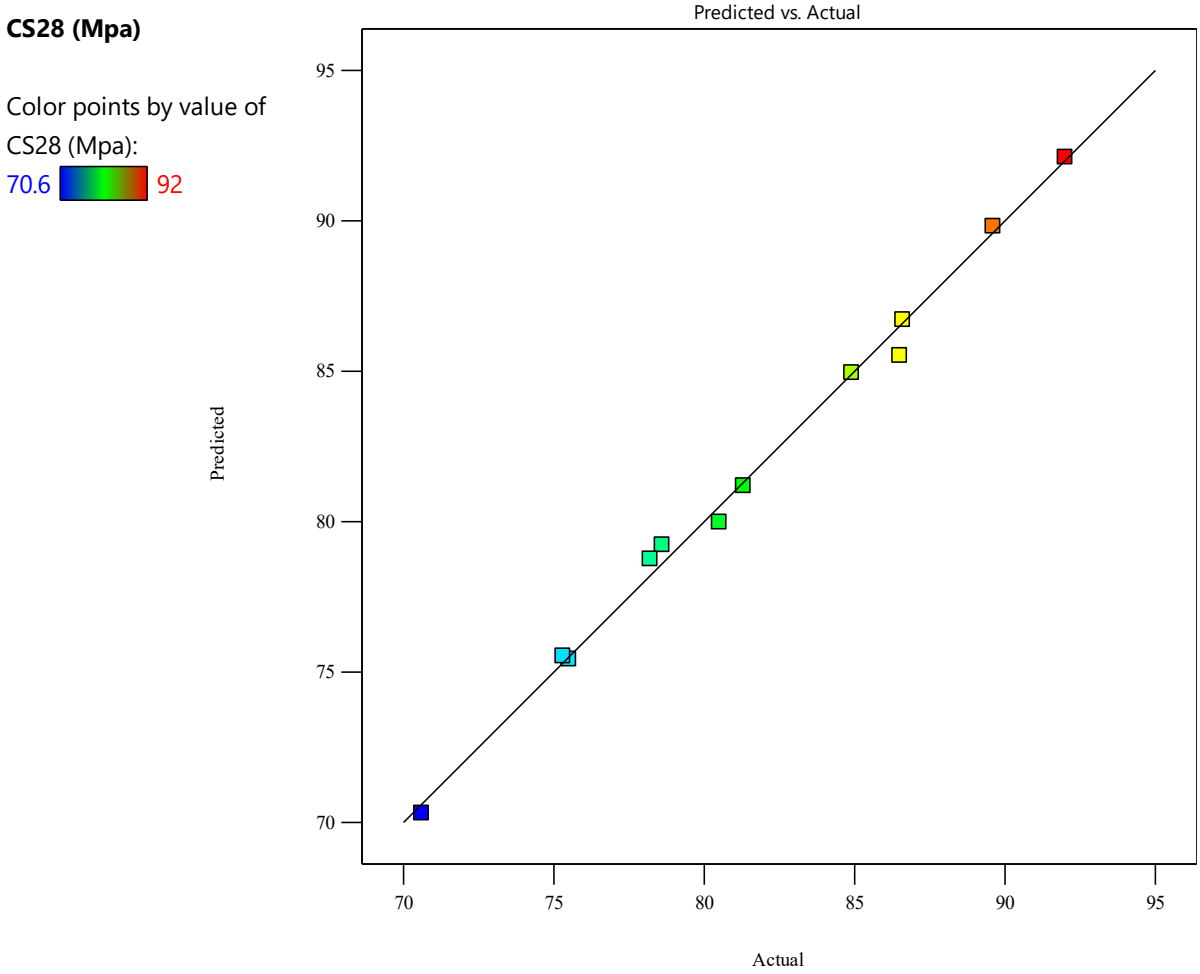

Figure 8. Predicted versus Actual Plot for Compressive Strength at 28 Days (CS28)

3.13. Effect of Model Factors and Interactions on CS28

Figure 9 illustrates the interaction and main effects plots with 95% confidence intervals for CS28, providing detailed insight into the influence of the studied factors on compressive strength at 28 days. The main effects plot shows that factor A (natural aggregate content) has a clear positive influence on CS28, where increasing A leads to a consistent increase in compressive strength. This is evident from the upward trend of the response curve, indicating that higher natural aggregate content enhances the mechanical performance of the concrete matrix. In contrast, factor B (recycled aggregate content) exhibits a nearly flat response, indicating a negligible or statistically insignificant effect on CS28 within the studied range. The minimal slope confirms the limited contribution of recycled aggregate to strength development at 28 days. The treatment type (factor C) demonstrates a nonlinear effect, as indicated by the curvature of the response plot. This suggests that different treatment methods significantly influence CS28, and the presence of curvature confirms the contribution of quadratic terms (C^2) in the model. The relatively narrow 95% confidence intervals around the fitted lines indicate high precision in the estimated effects and low experimental variability. Additionally, the absence of strong interaction curvature between factors A and B suggests that their combined effect is limited, consistent with the ANOVA results.

Overall, **Figure 9** confirms that factor A is the dominant contributor, followed by factor C, while factor B has a minimal effect, validating the statistical findings and reinforcing the robustness of the developed quadratic model for CS28 prediction. The relatively low influence of recycled aggregate (B) can be attributed to its higher porosity and the presence of adhered mortar, which weaken the interfacial transition zone (ITZ). However, within the studied replacement range, this effect remained secondary compared to the dominant role of natural aggregate content and treatment conditions. Additionally, the applied treatment methods contributed to mitigating the adverse effects of recycled aggregates, reducing their overall impact on the responses.

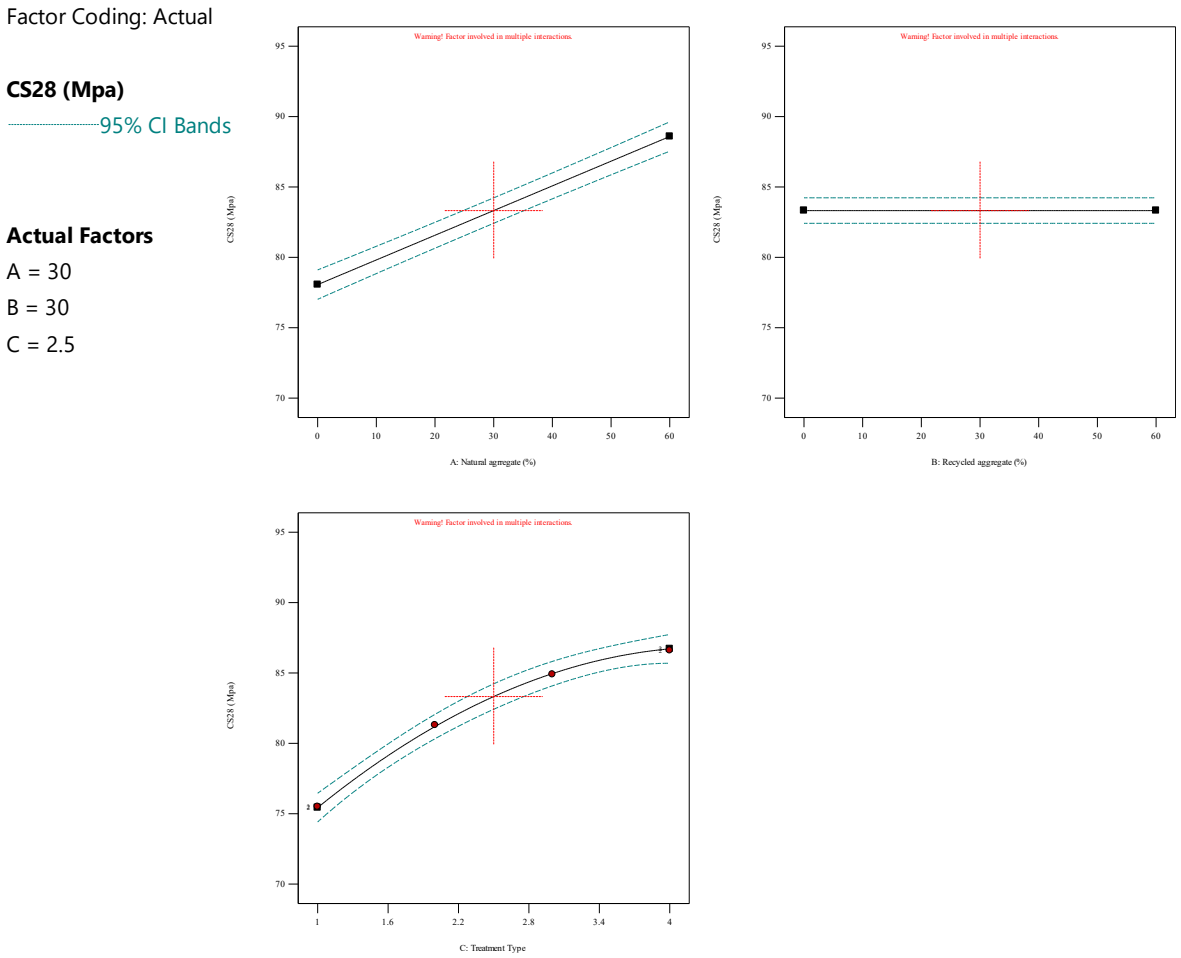

Figure 9. Interaction and Main Effects Plots with 95% Confidence Intervals for CS28

3.14. Response Surface Analysis for CS28

Figure 10 illustrates the three-dimensional response surface of CS28 as a function of factors A and B at a constant level of factor C, providing a comprehensive visualization of the combined effects of natural and recycled aggregate contents on compressive strength at 28 days. The response surface shows a clear increasing trend in CS28 values with increasing natural aggregate content (A), confirming its dominant positive influence on strength development. The surface gradient along the A-axis is relatively steep, indicating high sensitivity of CS28 to changes in natural aggregate proportion. In contrast, the variation along the recycled aggregate content (B) axis is comparatively minimal, as indicated by the relatively gentle slope of the surface. This suggests that factor B has a limited effect on CS28 within the studied range, consistent with the statistical insignificance observed in the ANOVA results. The response surface appears nearly planar with slight curvature, indicating that while linear effects dominate, minor quadratic contributions may still be present, particularly associated with other factors such as treatment type (C). The contour projection at the base further confirms the gradual and uniform increase in CS28 with increasing A, while showing limited variation with B. The absence of sharp curvature or interaction ridges indicates weak interaction between A and B. Overall, **Figure 10** confirms that natural aggregate content (A) is the primary controlling factor, while recycled aggregate (B) has a secondary influence, and the model provides a stable and reliable representation of CS28 behavior across the design space.

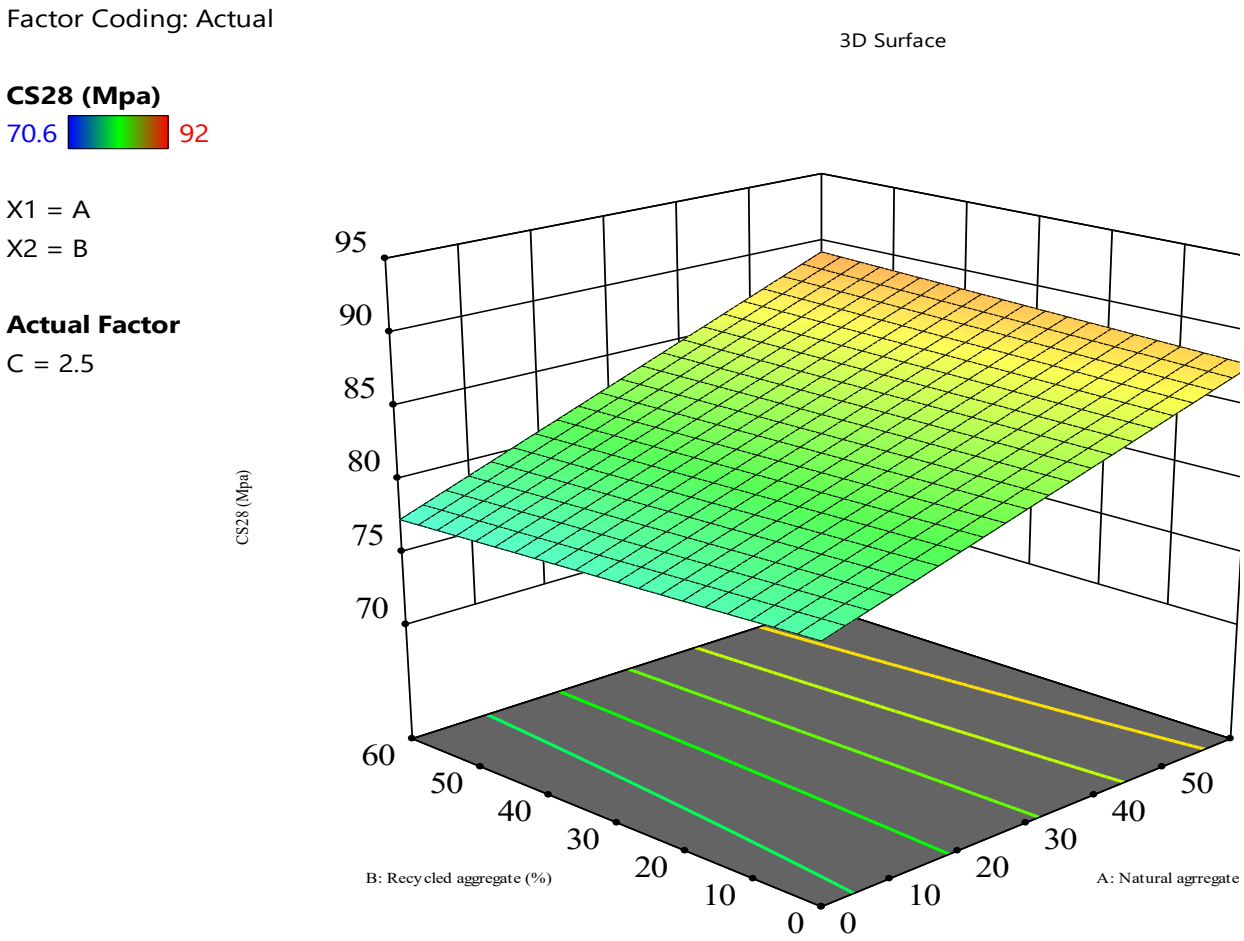

Figure 10. Three-Dimensional Response Surface of CS28 as a Function of A and B (C Constant)

3.15. Statistical Analysis of CS90 Response

Table 6 presents the ANOVA results for the quadratic model of compressive strength at 90 days (CS90), confirming the high statistical significance and robustness of the developed model. The model exhibits a very high F-value (209.51) with a p-value < 0.0001, indicating that the model is highly significant and that the probability of this result occurring due to random noise is negligible. Among the studied factors, treatment type (C) is identified as the most influential parameter, with a sum of squares = 304.20 and an exceptionally high F-value = 527.88 ($p < 0.0001$), demonstrating its dominant role in controlling long-term compressive strength. This is followed by natural aggregate

content (A), which also shows a strong and statistically significant effect (SS = 279.66, F = 485.30, $p < 0.0001$). In contrast, recycled aggregate content (B) exhibits no contribution (SS = 0.0000), confirming its negligible individual effect on CS90 within the studied experimental range. Regarding interaction terms, AB ($p = 0.3582$) and AC ($p = 0.0756$) are statistically insignificant, indicating weak or negligible interaction effects between these factors. The quadratic term C^2 is statistically significant ($F = 28.75$, $p = 0.0017$), confirming the presence of curvature in the response and highlighting the importance of considering nonlinear effects of treatment type on CS90. Other quadratic terms show no contribution, reinforcing that curvature is primarily associated with factor C. The residual error is low (SS = 3.46), indicating minimal unexplained variability and high model accuracy. Overall, the ANOVA results demonstrate that the developed quadratic model for CS90 is statistically valid, with factors C and A being the primary contributors, while factor B and most interaction terms have negligible influence.

Table 6. Analysis of Variance (ANOVA) for the Quadratic Model of Compressive Strength at 90 Days (CS90, MPa)

Source	Sum of Squares	df	Mean Square	F-value	p-value
Model	603.65	5	120.73	209.51	< 0.0001
A-Natural agrregate (%)	279.66	1	279.66	485.30	< 0.0001
B-Recycled aggregate (%)	0.0000	0			
C-Treatment Type	304.20	1	304.20	527.88	< 0.0001
AB	0.5704	1	0.5704	0.9899	0.3582
AC	2.65	1	2.65	4.60	0.0756
C^2	16.57	1	16.57	28.75	0.0017
Residual	3.46	6	0.5763		
Cor Total	607.11	11			

3.16. Model Adequacy and Predictive Performance for CS90

Table 7 presents the fit statistics and model adequacy metrics for the CS90 response, confirming the high reliability and predictive strength of the developed quadratic model. The coefficient of determination ($R^2 = 0.9943$) indicates that 99.43% of the total variation in compressive strength at 90 days is explained by the model, reflecting an excellent fit. The adjusted R^2 (0.9896) is very close to the R^2 value, indicating that the model is not overfitted and that all included terms contribute meaningfully to the response. Furthermore, the predicted R^2 (0.9635) is in strong agreement with the adjusted R^2, with a difference well below 0.2, demonstrating strong predictive capability for new observations within the experimental domain. The standard deviation (0.7591) remains relatively low, indicating limited dispersion of residuals and high precision in prediction. Additionally, the coefficient of variation (C.V. = 0.8347%) is very small, confirming excellent reproducibility and consistency of the experimental results. The Adeq Precision value (47.1982) is substantially higher than the required minimum value of 4, indicating a very strong signal-to-noise ratio and confirming that the model is highly suitable for navigating the design space. Overall, Table 7 demonstrates that the quadratic model for CS90 is statistically robust, highly accurate, and reliable for prediction and optimization of compressive strength at later curing ages.

Table 7. Fit Statistics and Model Adequacy for CS90 Response

Std. Dev.	0.7591		**R^2**	0.9943
Mean	90.94		**Adjusted R^2**	0.9896
C.V. %	0.8347		**Predicted R^2**	0.9635
			Adeq Precision	47.1982

3.17. Residual Analysis and Model Validation for CS90

Figure 11 illustrates the normal probability plot of studentized residuals for the CS90 model, confirming the adequacy of the developed quadratic model in light of the statistical results presented in Table 6 and Table 7. The residuals are closely aligned along the straight reference line, indicating that they follow an approximately normal distribution, which is a key assumption for ANOVA validity. The majority of residuals lie within the range of −2 to +2, with no extreme outliers observed, which is consistent with the low standard deviation (0.7591) reported in Table 7. This reflects minimal deviation between experimental and predicted values and confirms the precision of the model. The linear alignment of points supports the high model significance indicated by the F-value (209.51) and p-value < 0.0001 in Table 6, demonstrating that the model error is random rather than systematic. Additionally, the absence of curvature

or clustering away from the diagonal confirms that the model properly captures the relationship between the independent variables and CS90. The strong agreement between statistical indicators R^2 = 0.9943, Adjusted R^2 = 0.9896, and Predicted R^2 = 0.9635 is further validated by the normal distribution of residuals observed in Figure 11. This confirms that the model is both accurate and predictive without overfitting. Moreover, the high Adeq Precision (47.1982) is supported by the uniform spread of residuals, indicating a strong signal-to-noise ratio and reliable model performance across the design space. Overall, Figure 11, in conjunction with Tables 6 and 7, confirms that the residuals are normally distributed, independent, and randomly scattered, thereby validating the robustness, accuracy, and predictive capability of the quadratic model for CS90.

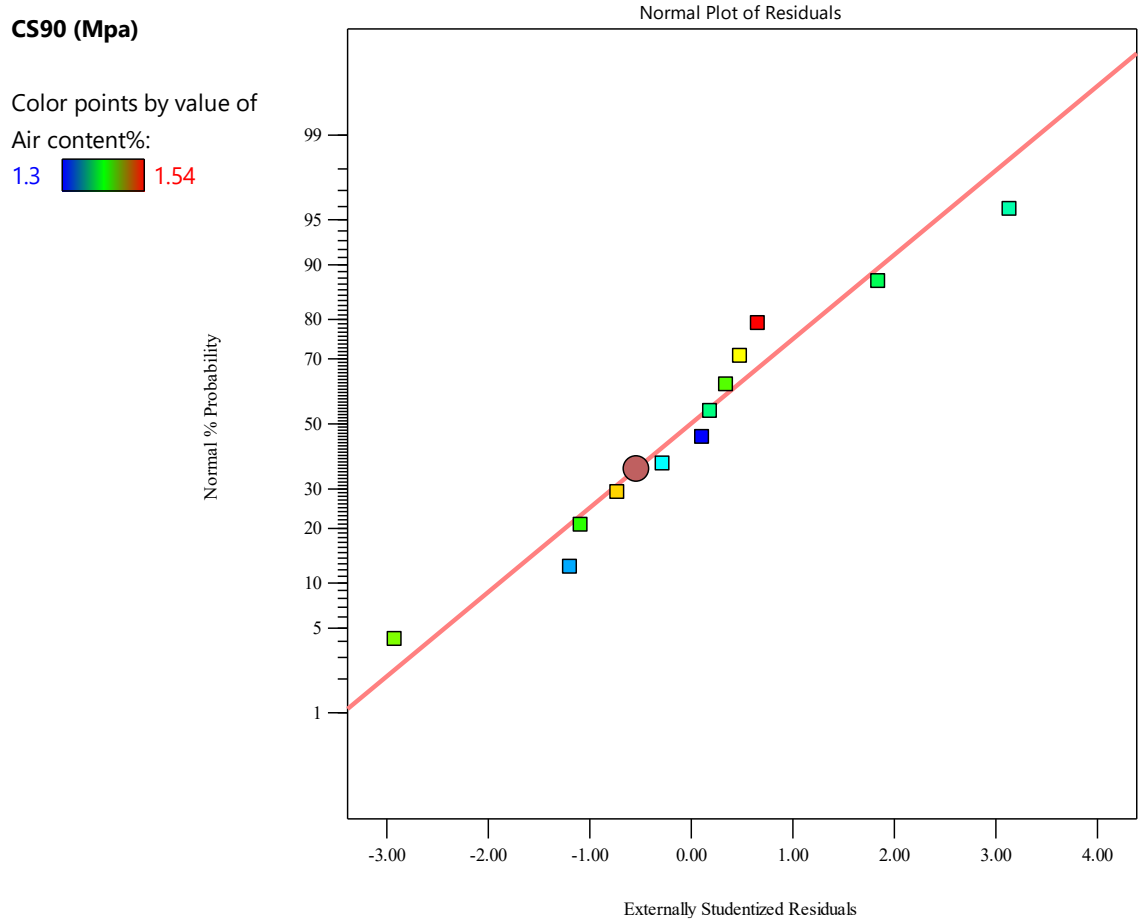

Figure 11. Normal Probability Plot of Residuals for CS90 Model

3.18. Residual Diagnostics for CS90 Model

Figure 12 illustrates the residuals versus predicted values for the CS90 model, providing a critical diagnostic check for homoscedasticity and model adequacy. The residuals are randomly scattered around the zero line without any clear pattern or systematic structure, indicating that the assumption of constant variance is satisfied. The residual values are distributed approximately within the range of -4 to +5, with the majority concentrated near zero. This spread is consistent with the relatively low standard deviation (0.7591) reported in Table 7, confirming that prediction errors are small and well-controlled. Importantly, no funnel-shaped pattern or curvature is observed, which indicates the absence of heteroscedasticity and confirms that the variance of errors remains constant across the predicted CS90 values. This behavior supports the validity of the regression model and aligns with the strong statistical significance indicated by the F-value (209.51) and p-value < 0.0001 in Table 6. Additionally, all data points fall within the control limits (approximately ±5), suggesting that there are no influential outliers or extreme deviations that could compromise the model's reliability. The consistency between this diagnostic plot and the statistical indicators R^2 = 0.9943, Adjusted R^2 = 0.9896, Predicted R^2 = 0.9635, and Adeq Precision = 47.1982 confirms that the model exhibits both high accuracy and stability. Overall, **Figure 12** validates that the residuals are randomly distributed with constant variance and no abnormal patterns, confirming the robustness and suitability of the developed quadratic model for CS90 prediction and optimization.

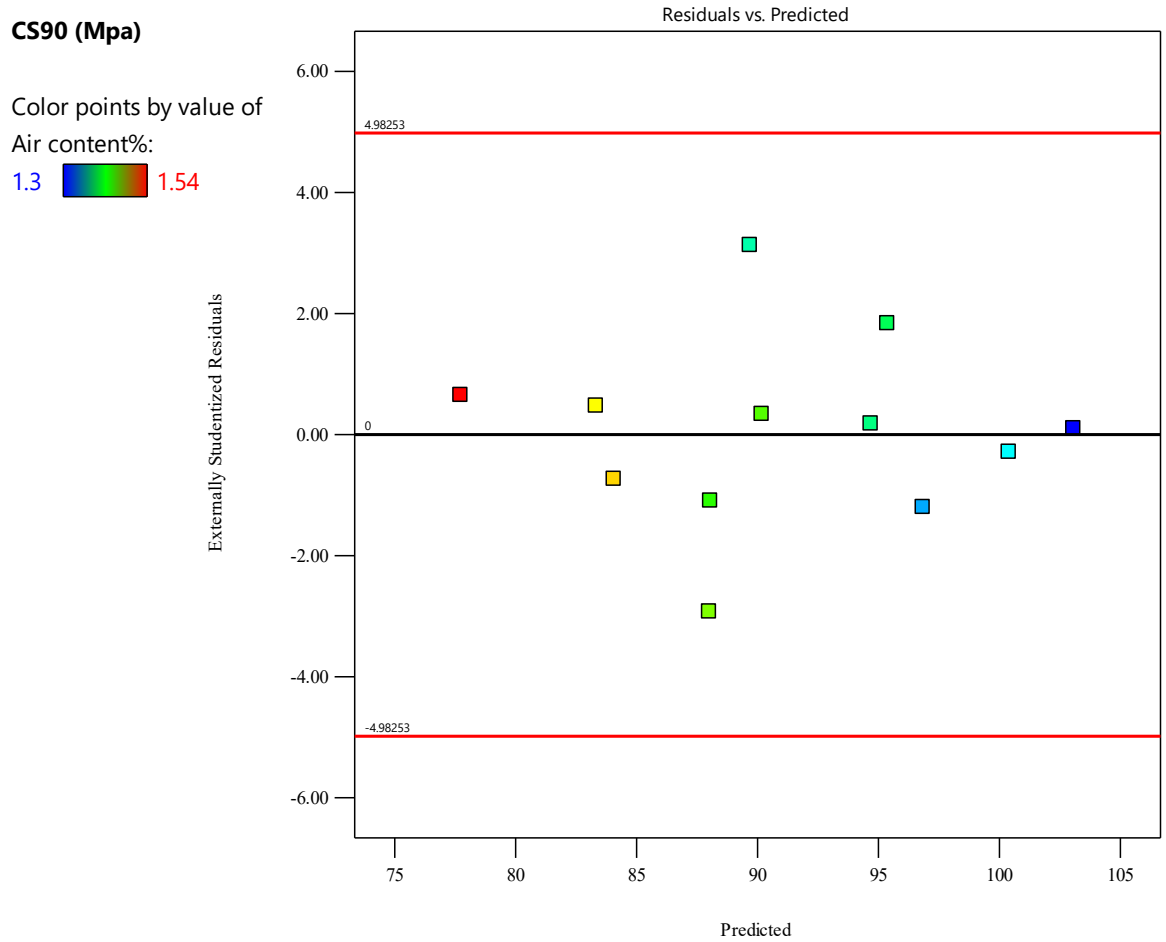

Figure 12. Residuals versus Predicted Values for CS90 Model Diagnostics

3.19. Residual Analysis for Run Order Stability of CS90 Model

Figure 13 illustrates the residuals versus run order for the CS90 model, providing a diagnostic assessment of independence and experimental stability across the sequence of runs. The residuals fluctuate randomly around the zero reference line, with no observable systematic trend, drift, or cyclic behavior, indicating that the independence assumption of the residuals is satisfied. The residual values range approximately from −3.0 to +3.2, with most observations concentrated within ±1.5, reflecting a relatively narrow dispersion. This behavior is consistent with the model's low residual variance (Std. Dev. = 0.7591) and supports the high predictive reliability indicated earlier. No sequential pattern, such as increasing or decreasing trends, is evident, confirming that there are no time-dependent effects, instrument drift, or experimental bias influencing the results. Additionally, all residuals lie well within the control limits (±5), indicating the absence of outliers or abnormal experimental runs. Minor fluctuations observed at specific run numbers (e.g., slight peaks near runs ~2 and ~12) remain within acceptable statistical limits and do not indicate instability. Instead, they reflect normal experimental variability. This randomness aligns with the strong statistical indicators of the model (R^2 = 0.9943, Adjusted R^2 = 0.9896, Predicted R^2 = 0.9635, Adeq Precision = 47.1982), confirming that the developed quadratic model is robust, stable, and free from autocorrelation issues. Overall, **Figure 13** verifies that the residuals are independently distributed with no underlying pattern, demonstrating that the experimental design and data acquisition process are reliable and that the CS90 model is suitable for prediction and optimization within the studied domain.

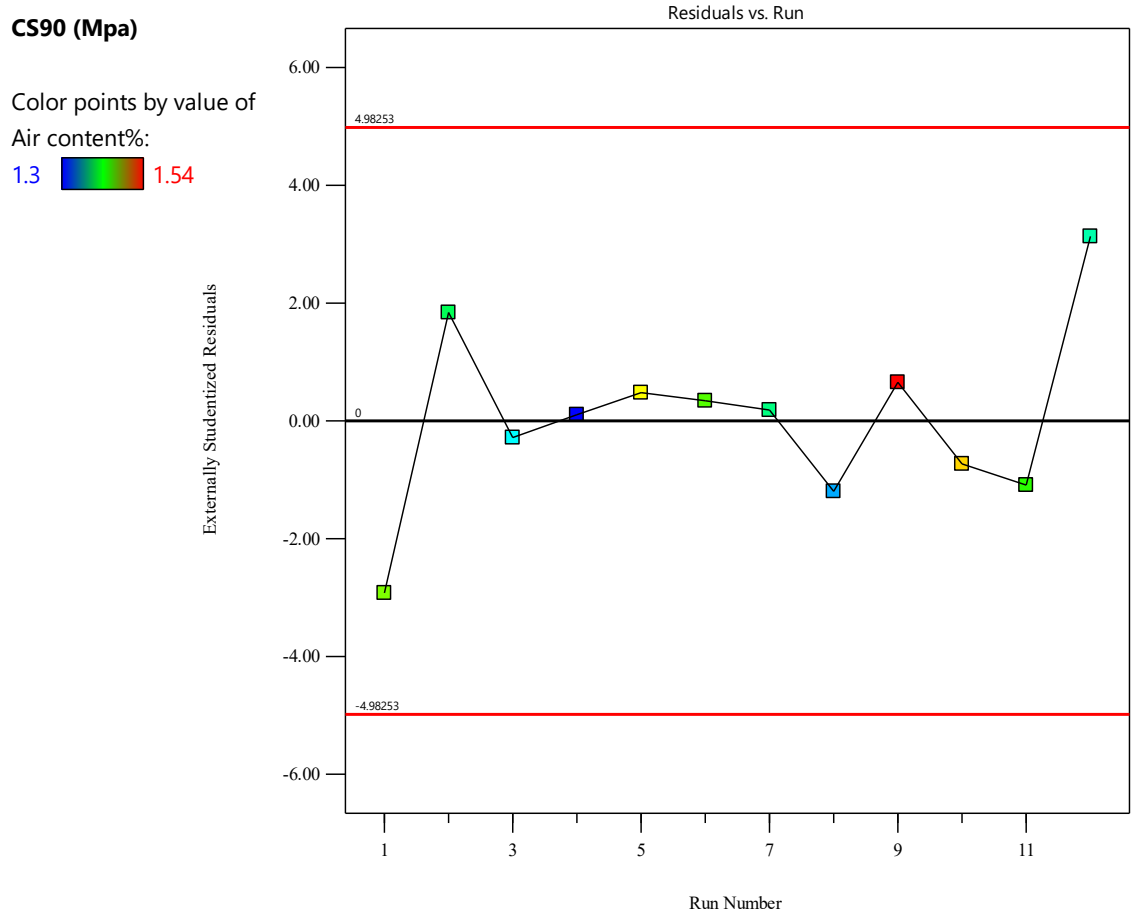

Figure 13. Residuals versus Run Order for CS90 Model Stability Assessment

3.20. Model Validation and Predictive Accuracy for CS90 Response

Figure 14 illustrates the predicted versus actual compressive strength values at 90 days (CS90), serving as a direct validation of the developed quadratic model's predictive capability. The data points are tightly aligned along the 45° reference line, indicating excellent agreement between experimentally measured and model-predicted values. The predicted values span approximately from 78 MPa to 104 MPa, closely matching the corresponding experimental results across the full design space. The near-perfect linear alignment confirms minimal deviation, with only negligible scatter around the diagonal, demonstrating high model fidelity. This strong agreement is quantitatively supported by the statistical metrics previously obtained, where $R^2 = 0.9943$ indicates that 99.43% of the variability in CS90 is explained by the model. Furthermore, the Adjusted R^2 (0.9896) and Predicted R^2 (0.9635) are in close agreement (difference < 0.03), confirming that the model is neither overfitted nor lacking predictive robustness. The uniform distribution of points along the diagonal without systematic bias (no clustering above or below the line) indicates that the model does not consistently overestimate or underestimate the response. Additionally, the color gradient (air content variation from 1.3% to 1.54%) shows no distortion in prediction accuracy across different operating conditions, further validating model generality. The high Adeq Precision value (47.1982) reinforces that the signal-to-noise ratio is exceptionally strong, ensuring reliable navigation within the design space. Overall, **Figure 14** confirms that the developed quadratic model provides highly accurate and reliable predictions for CS90, making it suitable for optimization and practical implementation in mix design and performance forecasting.

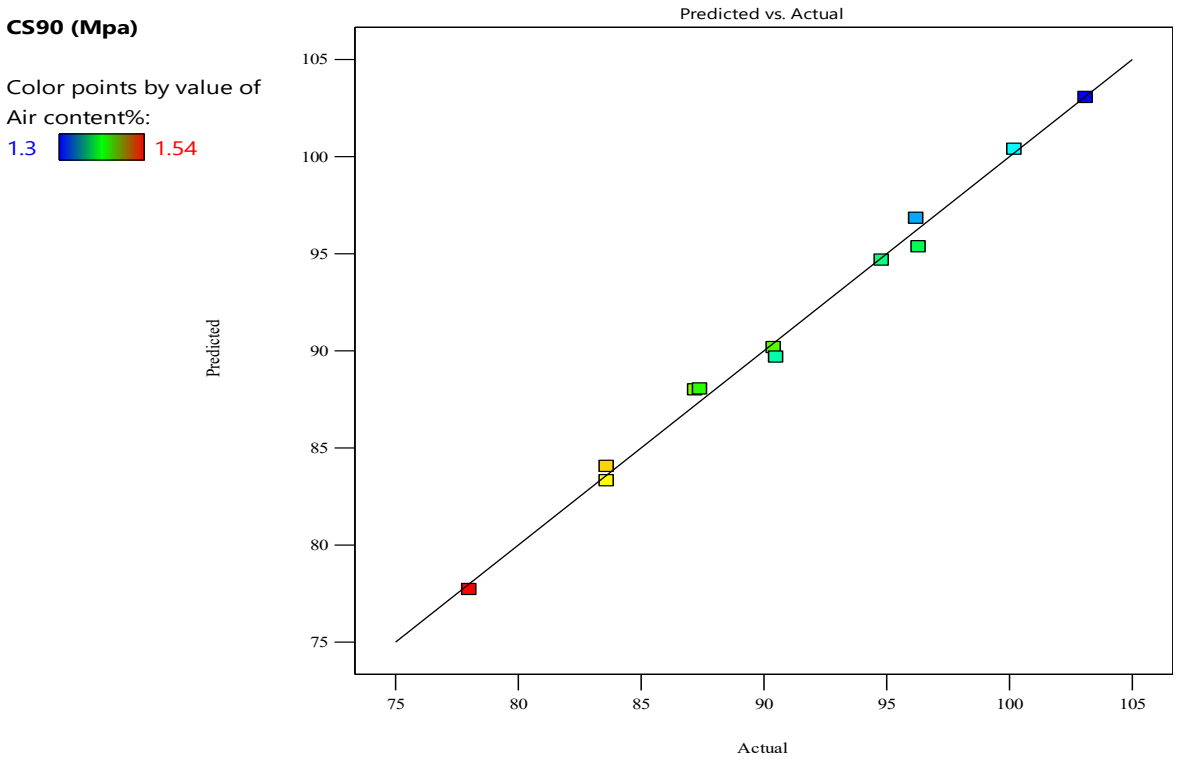

Figure 14. Predicted versus Actual Values for CS90 Model Accuracy Evaluation

3.21. Three-Dimensional Response Surface Analysis for CS90

Figure 15 illustrates the three-dimensional response surface of CS90 as a function of factors A (natural aggregate) and B (recycled aggregate), while factor C is held constant at 2.5, providing a comprehensive visualization of the combined effects of mixture composition on long-term compressive strength. The response surface shows a gradual increase in CS90 values from approximately 78 MPa to 103.1 MPa, indicating a strong dependence on the variation of factor A. The surface exhibits a clear positive gradient along the A-axis, confirming that increasing natural aggregate content significantly enhances compressive strength at 90 days. This observation is consistent with the high statistical contribution of factor A reported in ANOVA (Sum of Squares = 279.66, F-value = 485.30, $p < 0.0001$). In contrast, the surface appears relatively flat along the B-axis, indicating that the recycled aggregate content has a negligible or minimal effect on CS90. This aligns with the ANOVA results where factor B shows no significant contribution (Sum of Squares = 0.0000), confirming that its influence on long-term strength is statistically insignificant within the studied range. The smooth and nearly planar nature of the surface suggests that interaction effects between A and B are weak, which is further supported by the non-significant interaction term (AB: $p = 0.3582$). This implies that the effect of natural aggregate on compressive strength is largely independent of recycled aggregate variation. The contour projection beneath the surface reinforces this interpretation, showing nearly parallel contour lines, which indicate a dominant linear relationship with factor A and minimal curvature or interaction influence. Overall, **Figure 15** demonstrates that CS90 is primarily governed by the natural aggregate content, while recycled aggregate plays a secondary role. The model captures this behavior accurately, supported by strong statistical indicators ($R^2 = 0.9943$, Adjusted $R^2 = 0.9896$, Predicted $R^2 = 0.9635$), confirming its suitability for optimization and prediction of long-term compressive strength.

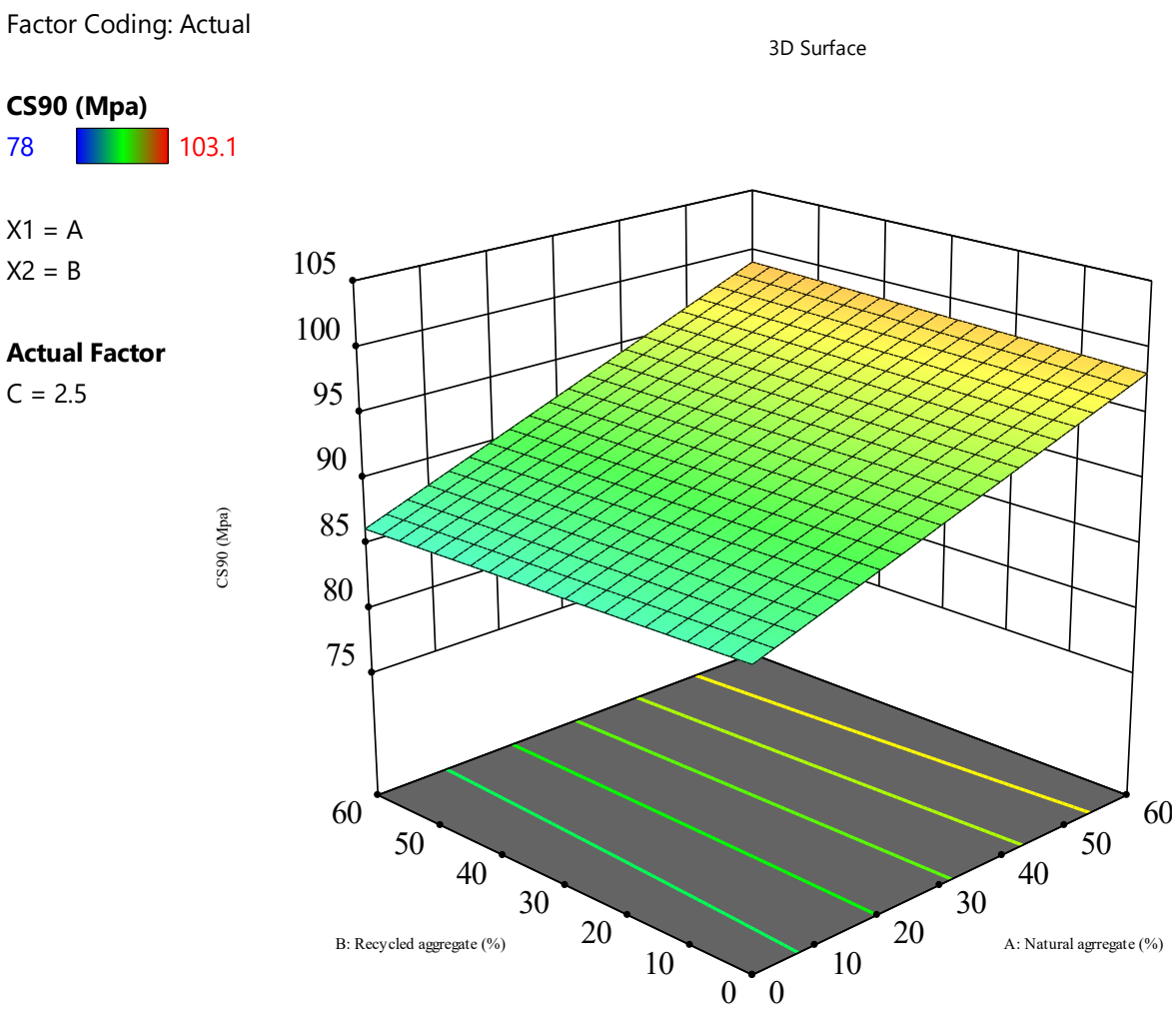

Figure 15. Three-Dimensional Response Surface of CS90 as a Function of A and B (C Constant)

3.22. Multi-Response Optimization and Contour Analysis

Figure 16 illustrates the multi-response optimization and contour plots for simultaneous performance evaluation, where the combined effects of factors A, B, and C on all responses are analyzed within a unified desirability framework. The color scale ranges from 0.000 (blue) to 1.000 (red), representing the desirability function, where higher values indicate more optimal conditions satisfying all response criteria simultaneously. The contour plots reveal that the optimal region is concentrated in the red–orange zone, indicating a narrow but well-defined design space where maximum performance is achieved. The plots show a strong gradient along factor A, with desirability increasing significantly as A increases. This confirms that natural aggregate content is the dominant controlling parameter across all responses, consistent with previous ANOVA findings where A exhibited the highest statistical significance. In contrast, the contour patterns along factor B are relatively uniform, indicating low sensitivity to recycled aggregate content, which aligns with its negligible contribution in earlier statistical analyses. The contour lines are mostly parallel with respect to B, confirming minimal interaction and weak influence. Factor C demonstrates a moderate nonlinear influence, as indicated by slight curvature in some contour plots. This behavior is consistent with the significance of quadratic terms (C^2) observed in the ANOVA results, suggesting that optimization requires careful tuning of treatment type rather than simple linear adjustment. The central region (highlighted by the marker) corresponds to the optimal operating condition, where all responses reach a balanced maximum desirability. The actual factor level shown ($C \approx 3.796$) indicates that the optimization algorithm converges toward an intermediate value of C rather than extreme levels, reflecting the presence of curvature effects. Overall, **Figure 16** confirms that simultaneous optimization is achievable within a constrained design space, primarily driven by factor A, moderately influenced by C, and minimally affected by B. The smooth and continuous contour transitions indicate a stable optimization landscape, validating the robustness of the developed quadratic models for multi-objective performance optimization.

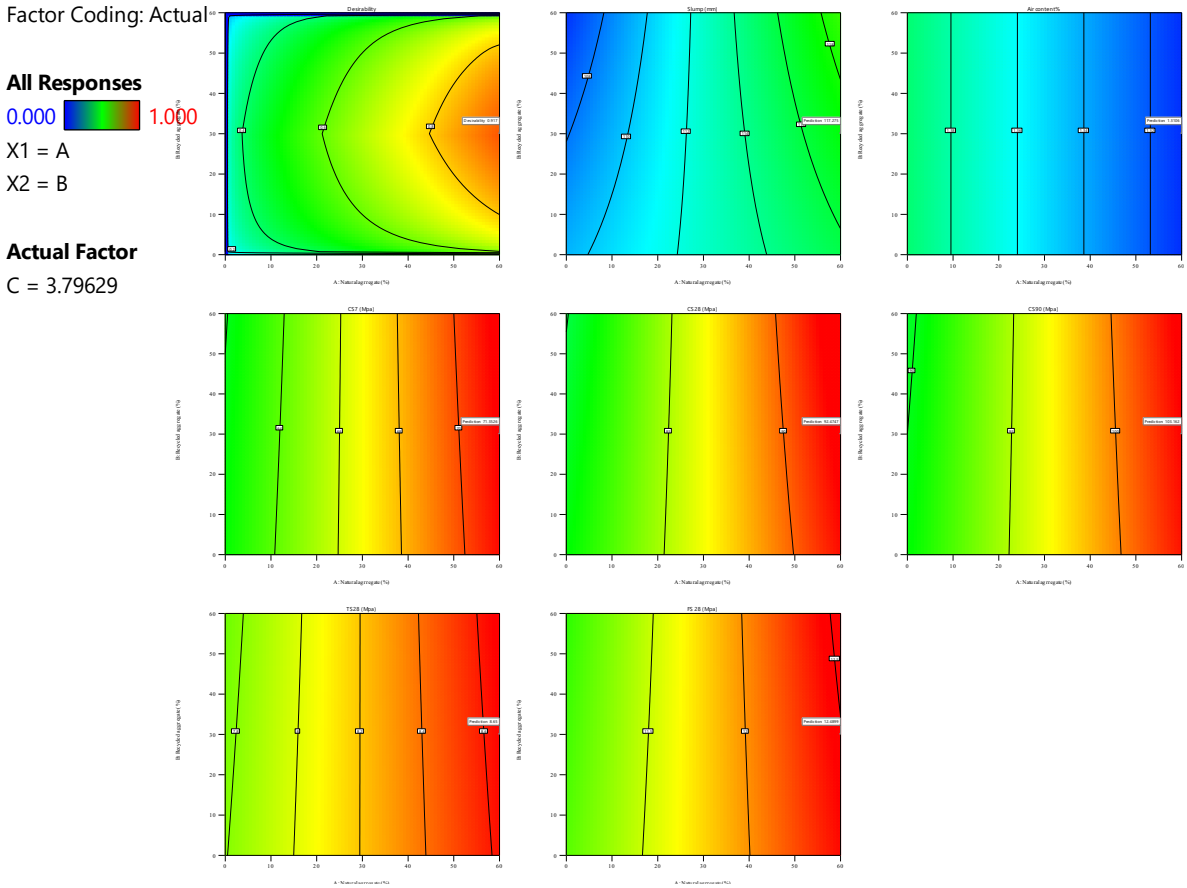

Figure 16. Multi-response optimization and contour plots for simultaneous performance evaluation, showing the interactions between factors: (A, B), (A, C), and (B, C).

4. CONCLUSION

This study systematically investigated the effects of natural aggregate (A), recycled aggregate (B), and treatment type (C) on the fresh and mechanical properties of concrete using Response Surface Methodology (RSM). The developed quadratic models demonstrated high statistical significance, with F-values of 342.27 for slump, 203.09 for CS7, and 209.51 for CS90 ($p < 0.0001$), confirming the robustness and reliability of the modeling approach. The results clearly indicated that natural aggregate content (A) is the most influential factor governing both workability and compressive strength across all curing ages. This was evidenced by its high contribution in ANOVA, with F-values reaching 547.60 (slump), 425.74 (CS7), and 485.30 (CS90). Treatment type (C) also exhibited a significant effect, particularly through its quadratic term (C^2), indicating nonlinear behavior and highlighting the importance of treatment optimization. In contrast, recycled aggregate content (B) showed negligible or statistically insignificant influence on most responses within the studied range, suggesting that its effect is secondary compared to A and C. The developed models exhibited excellent predictive capability, as confirmed by high coefficients of determination ($R^2 = 0.9965$ for slump, 0.9941 for CS7, and 0.9943 for CS90), along with strong agreement between adjusted and predicted R^2 values. The low standard deviation values (≤ 0.7591) and high adequate precision values (up to 60.336) further validated the accuracy and stability of the models. Residual analysis, including normal probability plots and residual distribution diagnostics, confirmed that the residuals are normally distributed, randomly scattered, and independent, with no evidence of heteroscedasticity or systematic bias. This validates the underlying assumptions of ANOVA and confirms the statistical adequacy of the developed models. Response surface and contour analyses demonstrated that increasing natural aggregate content significantly enhances both slump and compressive strength, while recycled aggregate content has minimal standalone impact. The interaction effects between variables were generally weak, except for a limited influence observed in specific cases. Multi-response optimization revealed that the optimal performance region is primarily governed by high levels of natural aggregate and intermediate treatment conditions, achieving desirability values approaching 1.0. Overall, the study provides a comprehensive statistical framework for understanding and

optimizing recycled aggregate concrete. The findings confirm that high-performance and sustainable concrete mixtures can be achieved through proper control of aggregate composition and treatment techniques, while minimizing the negative effects associated with recycled aggregates. From a practical perspective, the findings provide useful guidance for the design of sustainable concrete mixtures incorporating recycled aggregates. The results indicate that maintaining higher natural aggregate content combined with appropriate treatment of recycled aggregates can achieve a balance between mechanical performance and sustainability. This approach can be effectively applied in structural and non-structural concrete applications, contributing to resource conservation and waste reduction in the construction industry.

ACKNOWLEDGMENTS

The authors sincerely thank the referees, Associate Editor, and Editor-in-Chief for their valuable comments and suggestions, which have greatly improved this paper. DeepSeek is acknowledged for assistance with English language editing. The authors also thank the Department of Physics, College of Science, Sudan University of Science and Technology, for providing laboratory facilities and technical support. Valuable discussions with colleagues on perovskite synthesis and characterization are gratefully acknowledged.

DISCLOSURE STATEMENT

No potential conflict of interest was reported by the author(s).

REFERENCE

[1] Y. Moodi, S. Roohollah, A. Ghavidel, and M. Reza, “Using Response Surface Methodology and providing a modified model using whale algorithm for estimating the compressive strength of columns confined with FRP sheets,” Constr. Build. Mater., vol. 183, pp. 163–170, 2018, doi: 10.1016/j.conbuildmat.2018.06.081.

[2] Mostafa, S.A. and Alanazi, N., 2025. Comparative Analysis of Nano Zinc Oxide, Nano Silica Fume, and Nano Marble Powder as Cement Replacements in Self-Compacting Concrete. *Advanced Multidisciplinary Engineering Journal (AMEJ)*, *1*(2), pp.31-43.

[3] H. He, S. Cheng, Y. Chen, and B. Lan, “Compression performance analysis of multi-scale modified concrete based on response surface method,” Case Stud. Constr. Mater., vol. 17, no. July, p. e01312, 2022, doi: 10.1016/j.cscm.2022.e01312.

[4] P. Rattanachu, P. Toolkasikorn, W. Tangchirapat, P. Chindaprasirt, and C. Jaturapitakkul, "Performance of recycled aggregate concrete with rice husk ash as cement binder," *Cement and Concrete Composites,* vol. 108, p. 103533, 2020.

[5] Mostafa, S.A. and AlAteah, A.H., 2025. Sustainable Ultra-High-Performance Concrete: Incorporating Nano-Eggshell Waste for Improved Strength and Durability. *Advanced Multidisciplinary Engineering Journal (AMEJ)*, *1*(1), pp.1-8.

[6] B. A. Tayeh, I. Almeshal, H. M. Magbool, H. Alabduljabbar, and R. Alyousef, "Performance of sustainable concrete containing different types of recycled plastic," *Journal of Cleaner Production,* vol. 328, 2021.

[7] W. Ahmed and C. W. Lim, "Production of sustainable and structural fiber reinforced recycled aggregate concrete with improved fracture properties: A review," *Journal of Cleaner Production,* vol. 279, 2021.

[8] X. Ye *et al.*, "Enhancing self-healing of asphalt mixtures containing recycled concrete aggregates and reclaimed asphalt pavement using induction heating," vol. 439, p. 137361, 2024.

[9] I. S. Agwa, S. A. Mostafa, M. H. Abd-Elrahman, and M. J. J. o. B. E. Amin, "Effect of Recycled Aggregate Treatment Using Fly Ash, Palm Leaf Ash, and Silica Fume Slurries on the Mechanical and Transport Properties of High-Strength Concrete," p. 113292, 2025.

[10] A. Riyanto, S. Sembiring, S. Husain, R. S. Karimah, and I. Firdaus, "Rietveld analysis of geopolymer prepared from amorphous rice husk silica with different thermal treatment," *Journal of Physics: Conference Series,* vol. 1751, no. 1, 2021.

[11] A. H. Jagaba *et al.*, "A Systematic Literature Review on Waste-to-Resource Potential of Palm Oil Clinker for Sustainable Engineering and Environmental Applications," *Materials (Basel),* vol. 14, no. 16, Aug 9 2021.

[12] S.-J. Sammut *et al.*, "Multi-omic machine learning predictor of breast cancer therapy response," vol. 601, no. 7894, pp. 623-629, 2022.

[13] K. Khan, S. Khan, M. Ahmed, W. Ahmed, S. Khan, and G. J. S. C. Zaman, "Multi-response optimization of carbon-nanotubes concrete: Study on mechanical properties and durability behaviors," vol. 26, no. 6, pp. 7795-7815, 2025.

[14] G. Murali, S. R. Abid, K. Karthikeyan, M. K. Haridharan, M. Amran, and A. Siva, "Low-velocity impact response of novel prepacked expanded clay aggregate fibrous concrete produced with carbon nanotube, glass fiber mesh and steel fiber," *Construction and Building Materials,* vol. 284, 2021.

[15] B. Joshi, X. Li, Y. Oz, J. Wang, X. Shan, and Y. J. C. P. B. E. Mo, "Effects of fiber dosage, loading orientation and stress on frequency response of enhanced Carbon Nano-Fiber Aggregates," vol. 225, p. 109257, 2021.

[16] E. Ghafari, H. Costa, E. J. C. Júlio, and B. Materials, "RSM-based model to predict the performance of self-compacting UHPC reinforced with hybrid steel micro-fibers," vol. 66, pp. 375-383, 2014.

[17] A. Hammoudi, K. Moussaceb, C. Belebchouche, and F. Dahmoune, "Comparison of artificial neural network (ANN) and response surface methodology (RSM) prediction in compressive strength of recycled concrete aggregates," *Construction and Building Materials,* vol. 209, pp. 425-436, 2019.

[18] Q. Li, L. Cai, Y. Fu, H. Wang, Y. J. C. Zou, and B. Materials, "Fracture properties and response surface methodology model of alkali-slag concrete under freeze–thaw cycles," vol. 93, pp. 620-626, 2015.

[19] I. Ferdosian, A. J. C. Camões, and C. Composites, "Eco-efficient ultra-high performance concrete development by means of response surface methodology," vol. 84, pp. 146-156, 2017.

[20] A. Arora, Y. Yao, B. Mobasher, and N. Neithalath, "Fundamental insights into the compressive and flexural response of binder- and aggregate-optimized ultra-high performance concrete (UHPC)," *Cement and Concrete Composites,* vol. 98, pp. 1-13, 2019.

[21] M. A. Mosaberpanah, O. Eren, and A. R. Tarassoly, "The effect of nano-silica and waste glass powder on mechanical, rheological, and shrinkage properties of UHPC using response surface methodology," *Journal of Materials Research and Technology,* vol. 8, no. 1, pp. 804-811, 2019.

[22] A. A. Mahmoud, A. A. El-Sayed, A. M. Aboraya, I. N. Fathy, M. A. Abouelnour, and I. M. J. S. R. Nabil, "Influence of sustainable waste granite, marble and nano-alumina additives on ordinary concretes: a physical, structural, and radiological study," vol. 14, no. 1, p. 22011, 2024.

[23] S. Indhumathi, S. P. Kumar, M. J. C. Pichumani, and B. Materials, "Reconnoitring principles and practice of Modified Andreasen and Andersen particle packing theory to augment Engineered cementitious composite," vol. 353, p. 129106, 2022.

[24] A. Essam, S. A. Mostafa, M. Khan, A. M. J. C. Tahwia, and B. Materials, "Modified particle packing approach for optimizing waste marble powder as a cement substitute in high-performance concrete," vol. 409, p. 133845, 2023.

[25] M. A. Arab, L. Hadji, M. I. Al Biajawi, and M. M. J. A. M. E. J. Eldin, "Optimization of Recycled Asphalt Aggregate Treatment for High-Strength Prepacked Concrete: Influence of Immersion Duration and Replacement Ratio," vol. 2, no. 1, pp. 1-16, 2026.

[26] H. Dilbas and Ö. Çakır, "Influence of basalt fiber on physical and mechanical properties of treated recycled aggregate concrete," *Construction and Building Materials,* vol. 254, p. 119216, 2020.

[27] P. Nuaklong, P. Jongvivatsakul, T. Pothisiri, V. Sata, and P. Chindaprasirt, "Influence of rice husk ash on mechanical properties and fire resistance of recycled aggregate high-calcium fly ash geopolymer concrete," *Journal of Cleaner Production,* vol. 252, p. 119797, 2020.

[28] S.A. Mostafa and M.S. Hammad, 2025. Optimizing Pelargonium Ash as a Partial Cement Replacement in High-Strength Self-Compacting Concrete: Mechanical and Durability Aspects. *Advanced Multidisciplinary Engineering Journal (AMEJ)*, *1*(1), pp.9-18.

[29] I.S. Agwa, S.A. Mostafa, M.H. Abd-Elrahman, and M. Amin, 2025. Effect of recycled aggregate treatment using fly ash, palm leaf ash, and silica fume slurries on the mechanical and transport properties of high-strength concrete. *Journal of Building Engineering*, *111*, p.113292.